



INSTITUT
POLYTECHNIQUE
DE PARIS

inria



Hybrid High-Order Methods for the Numerical Simulation of Elasto-Acoustic Wave Propagation

Romain Mottier^{†‡§}

PhD in Applied Mathematics

Advisors: Alexandre Ern^{†‡}, Laurent Guillot[§]

[†] CERMICS, Ecole des Ponts, F-77455 Marne la Vallée cedex 2

[‡] SERENA Project-Team, INRIA Paris, F-75647 Paris France

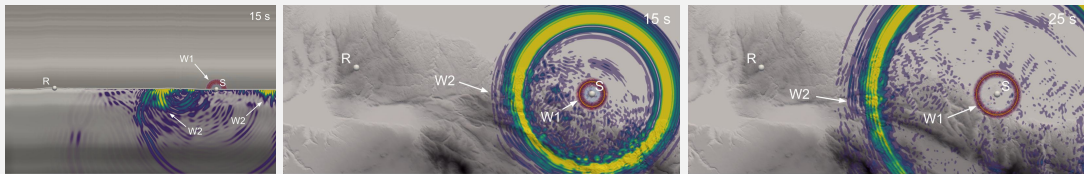
[§] CEA, DAM, DIF, F-91297 Arpajon, France

Context & motivations

- Mechanical waves: Acoustic (fluid) / Elastic (solid)
- Applications: **Geophysics**, Medical imaging (elastography), Non-destructive testing etc...

Context & motivations

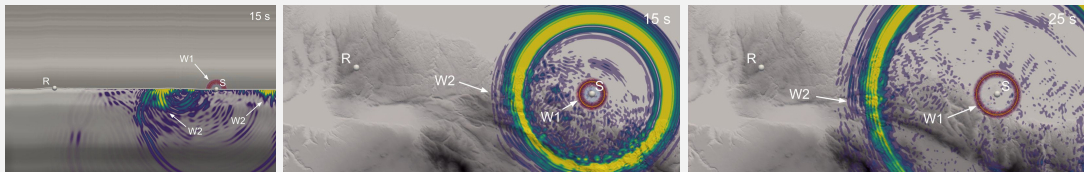
- Mechanical waves: Acoustic (fluid) / Elastic (solid)
- Applications: **Geophysics**, Medical imaging (elastography), Non-destructive testing etc...
- Example: Seismic monitoring of Beyrouth explosion (@Gaël Burgos - CEA/DAM/DASE)



- Objectives: **Detection, Localization, Source characterization**

Context & motivations

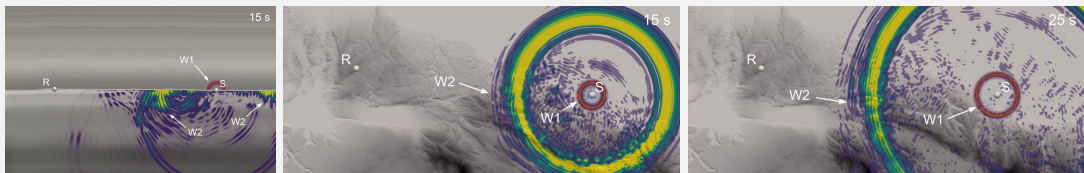
- Mechanical waves: Acoustic (fluid) / Elastic (solid)
- Applications: **Geophysics**, Medical imaging (elastography), Non-destructive testing etc...
- Example: Seismic monitoring of Beyrouth explosion (@Gaël Burgos - CEA/DAM/DASE)



- Objectives: **Detection, Localization, Source characterization**
- **Goal:** Simulate accurately elasto-acoustic waves propagation in **heterogeneous** and **complex** domains
 - ▶ System of the form: $\mathcal{M}\ddot{\mathbf{U}} + \mathcal{K}\mathbf{U} = \mathbf{F}$ **OR**
$$\begin{bmatrix} \mathcal{M}_U & 0 \\ 0 & \mathcal{M}_\Sigma \end{bmatrix} \begin{bmatrix} \dot{\mathbf{U}} \\ \dot{\Sigma} \end{bmatrix} + \begin{bmatrix} \mathcal{K}_{UU} & \mathcal{K}_{U\Sigma} \\ \mathcal{K}_{\Sigma U} & \mathcal{K}_{\Sigma\Sigma} \end{bmatrix} \begin{bmatrix} \mathbf{U} \\ \Sigma \end{bmatrix} = \begin{bmatrix} \mathbf{0} \\ \mathbf{F} \end{bmatrix}$$

Context & motivations

- Mechanical waves: Acoustic (fluid) / Elastic (solid)
- Applications: **Geophysics**, Medical imaging (elastography), Non-destructive testing etc...
- Example: Seismic monitoring of Beyrouth explosion (@Gaël Burgos - CEA/DAM/DASE)



- Objectives: **Detection, Localization, Source characterization**
- **Goal:** Simulate accurately elasto-acoustic waves propagation in **heterogeneous** and **complex** domains
 - ▶ System of the form:
 - ▶ Discretization: **Hybrid High-Order methods** in space & **Runge–Kutta schemes** in time

$$\begin{bmatrix} \mathcal{M}_U & 0 \\ 0 & \mathcal{M}_\Sigma \end{bmatrix} \begin{bmatrix} \dot{\mathbf{U}} \\ \dot{\Sigma} \end{bmatrix} + \begin{bmatrix} \mathcal{K}_{UU} & \mathcal{K}_{U\Sigma} \\ \mathcal{K}_{\Sigma U} & \mathcal{K}_{\Sigma\Sigma} \end{bmatrix} \begin{bmatrix} \mathbf{U} \\ \Sigma \end{bmatrix} = \begin{bmatrix} 0 \\ \mathbf{F} \end{bmatrix}$$

Table of Contents

I - State of the art

Table of Contents

I - State of the art

II - HHO for elasto-acoustic coupling

-  R. Mottier, A. Ern, R. Khot, L. Guillot (2025). Accepted in M2AN
Hybrid high-order methods for elasto-acoustic wave propagation in the time domain
-  R. Mottier, A. Ern, L. Guillot (2025). Submitted to CMAME
Elasto-acoustic wave propagation in geophysical media using hybrid high-order methods on general meshes

Table of Contents

I - State of the art

II - HHO for elasto-acoustic coupling

-  R. Mottier, A. Ern, R. Khot, L. Guillot (2025). Accepted in M2AN
Hybrid high-order methods for elasto-acoustic wave propagation in the time domain
-  R. Mottier, A. Ern, L. Guillot (2025). Submitted to CMAME
Elasto-acoustic wave propagation in geophysical media using hybrid high-order methods on general meshes

III - HHO on unfitted meshes: stabilization by polynomial extension

-  E. Burman, A. Ern, R. Mottier (2025). Submitted to SINUM
Unfitted hybrid high-order methods stabilized by polynomial extension for elliptic interface problems

Table of Contents

I - State of the art

II - HHO for elasto-acoustic coupling

-  R. Mottier, A. Ern, R. Khot, L. Guillot (2025). Accepted in M2AN
Hybrid high-order methods for elasto-acoustic wave propagation in the time domain
-  R. Mottier, A. Ern, L. Guillot (2025). Submitted to CMAME
Elasto-acoustic wave propagation in geophysical media using hybrid high-order methods on general meshes

III - HHO on unfitted meshes: stabilization by polynomial extension

-  E. Burman, A. Ern, R. Mottier (2025). Submitted to SINUM
Unfitted hybrid high-order methods stabilized by polynomial extension for elliptic interface problems

IV - Conclusion and perspectives

Table of Contents

I - State of the art

- I.1 Numerical methods for wave propagation
- I.2 Hybrid nonconforming methods: HDG/HHO
- I.3 Further insight into HHO

I.1. Numerical methods for wave propagation

- **Finite Differences (FD):** Ideal for simple geometries  [van Vossen, Robertsson, Chapman \(2002\)](#)

I.1. Numerical methods for wave propagation

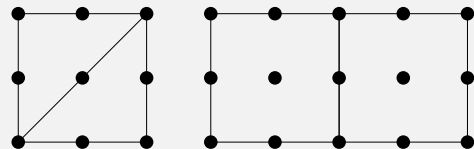
- Finite Differences (FD): Ideal for simple geometries  van Vossen, Robertsson, Chapman (2002)

- Finite Element Methods (cG)  Marfurt (1984)  Basabe, Sen (2007)

✓ Allow for unstructured meshes

✗ Non-local polynomial bases

✗ Non-diagonal mass matrix:
Mass lumping required for explicit schemes



I.1. Numerical methods for wave propagation

- **Finite Differences (FD):** Ideal for simple geometries  van Vossen, Robertsson, Chapman (2002)

- **Finite Element Methods (cG)**  Marfurt (1984)

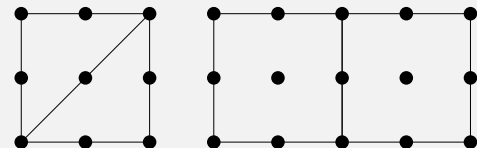
-  Basabe, Sen (2007)

✓ Allow for unstructured meshes

✗ Non-local polynomial bases

✗ Non-diagonal mass matrix:

Mass lumping required for explicit schemes



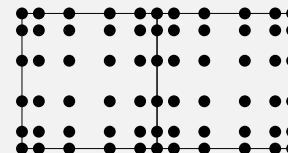
- **Spectral Element Method (SEM)**  Patera (1984)  Komatitsch, Vilotte (1998)  Cohen (2002)

► Quadrature points: tensorized GLL nodes

✓ Diagonal mass matrix

✓ Parallelizable and scalable for HPC applications

✗ Mainly quadrangular/hexahedral meshes



■ Main issue: Complex meshes for realistic geological structures

- ▶ Difficult to use only one simple shapes
- ▶ Presence of hanging nodes due to independent subdomain meshes

■ Main issue: Complex meshes for realistic geological structures

- ▶ Difficult to use only one simple shapes
- ▶ Presence of hanging nodes due to independent subdomain meshes

■ Solution: Polytopal discretization methods

QUADRANGLES



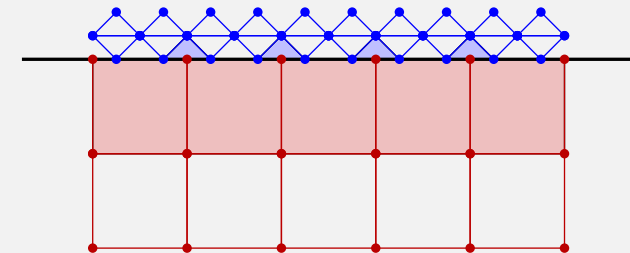
HEXAGONS



TRIANGLES



QUADRANGLES



■ Main issue: Complex meshes for realistic geological structures

- ▶ Difficult to use only one simple shapes
- ▶ Presence of hanging nodes due to independent subdomain meshes

■ Solution: Polytopal discretization methods

QUADRANGLES



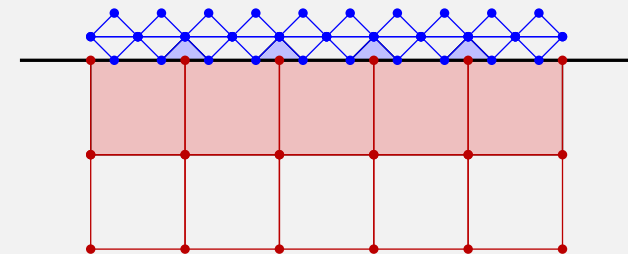
HEXAGONS



TRIANGLES



QUADRANGLES



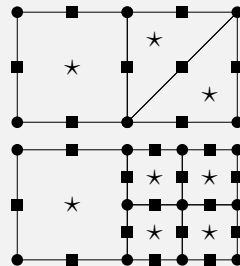
■ Two possibilities:

- ▶ H^1 -conforming polytopal methods: **Virtual Element Methods (VEM)**
- ▶ Nonconforming methods: **class of discontinuous Galerkin methods**

■ Virtual Element Methods (VEM)

- ❑ da Veiga, Brezzi, Cangiani, Manzini, Marini, Russo (2013)
- ❑ Dassi, Fumagalli, Mazzieri, Scotti, Vacca (2022)
- ❑ Wriggers, Junker (2024)

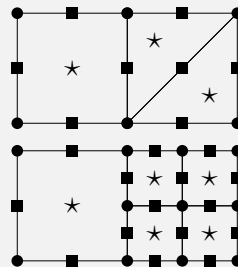
✖ Same issue as cG: **Non-diagonal mass matrix**
(dofs attached to low-dimensional mesh entities)



■ Virtual Element Methods (VEM)

- ❑ da Veiga, Brezzi, Cangiani, Manzini, Marini, Russo (2013)
- ❑ Dassi, Fumagalli, Mazzieri, Scotti, Vacca (2022)
- ❑ Wriggers, Junker (2024)

✖ Same issue as cG: Non-diagonal mass matrix
(dofs attached to low-dimensional mesh entities)



■ Discontinuous Galerkin methods (dG)

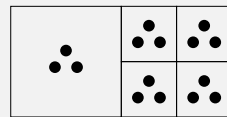
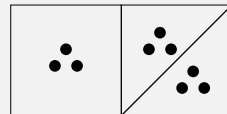
- ❑ Baker (1976) ❑ Wheeler (1978) ❑ Arnold (1982)
- ❑ Grote, Schneebeli, Schötzau (2006)
- ❑ Antonietti, Bonaldi, Mazzieri (2020)

✓ Block-diagonal mass matrix

✖ More dofs than cG

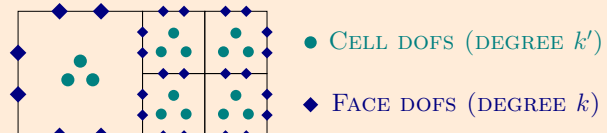
✓ Compact stencil (HPC)

✖ **Stabilization:** Face-based
(Minimal value)



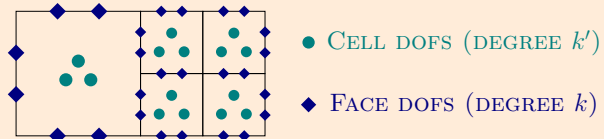
I.2. Hybrid Nonconforming Methods HDG/HHO

Idea: Additional unknowns attached to mesh faces



I.2. Hybrid Nonconforming Methods HDG/HHO

Idea: Additional unknowns attached to mesh faces



Hybridizable discontinuous Galerkin (HDG)

Hybrid High-Order (HHO)

■ Seminal papers:



Cockburn, Gopalakrishnan, Lazarov (2009)



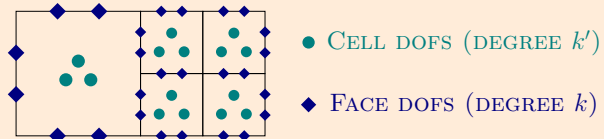
Di Pietro, Ern, Lemaire (2014)



Di Pietro, Ern (2015)

I.2. Hybrid Nonconforming Methods HDG/HHO

Idea: Additional unknowns attached to mesh faces



Hybridizable discontinuous Galerkin (HDG)

■ Seminal papers:

Cockburn, Gopalakrishnan, Lazarov (2009)

■ Wave propagation:

Stanglmeier, Nguyen, Peraire, Cockburn (2016)

Kronbichler, Schoeder, Müller, Wall (2016)

Barucq, Rouxelin, Tordeux (2023)

Hybrid High-Order (HHO)

Di Pietro, Ern, Lemaire (2014)

Di Pietro, Ern (2015)

Burman, Duran, Ern, Steins (2021)

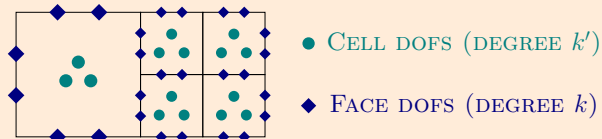
Burman, Duran, Ern (2022a)

Steins, Ern, Jamond, Drui (2023)

Ern, Steins (2024)

I.2. Hybrid Nonconforming Methods HDG/HHO

Idea: Additional unknowns attached to mesh faces



Hybridizable discontinuous Galerkin (HDG)

Hybrid High-Order (HHO)

- Seminal papers:
 - Cockburn, Gopalakrishnan, Lazarov (2009)
 - Di Pietro, Ern, Lemaire (2014)
- Wave propagation:
 - Stanglmeier, Nguyen, Peraire, Cockburn (2016)
 - Kronbichler, Schoeder, Müller, Wall (2016)
 - Burman, Duran, Ern, Steins (2021)
 - Barucq, Rouxelin, Tordeux (2023)
 - Burman, Duran, Ern (2022a)
 - Steins, Ern, Jamond, Drui (2023)
 - Ern, Steins (2024)
- HHO \equiv HDG but with different viewpoints
 - ▶ Approximate $(-\nabla u, u, u|_{\mathcal{F}})$
 - ▶ Gradient is part of unknowns
 - ▶ Stabilization in numerical flux
 - ▶ Approximate $\hat{u} := (u, u|_{\mathcal{F}})$
 - ▶ Explicit gradient reconstruction
 - ▶ Explicit stabilization

I.2. Hybrid Nonconforming Methods HDG/HHO

Idea: Additional unknowns attached to mesh faces



Hybridizable discontinuous Galerkin (HDG)

Hybrid High-Order (HHO)

- Seminal papers:
 - Cockburn, Gopalakrishnan, Lazarov (2009)
 - Di Pietro, Ern, Lemaire (2014)
- Wave propagation:
 - Stanglmeier, Nguyen, Peraire, Cockburn (2016)
 - Burman, Duran, Ern, Steins (2021)
 - Kronbichler, Schoeder, Müller, Wall (2016)
 - Burman, Duran, Ern (2022a)
 - Barucq, Rouxelin, Tordeux (2023)
 - Steins, Ern, Jamond, Drui (2023)
- HHO \equiv HDG but with different viewpoints
 - ▶ Approximate $(-\nabla u, u, u|_{\mathcal{F}})$
 - ▶ Approximate $\hat{u} := (u, u|_{\mathcal{F}})$
 - ▶ Gradient is part of unknowns
 - ▶ Explicit gradient reconstruction
 - ▶ Stabilization in numerical flux
 - ▶ Explicit stabilization

HHO \equiv HDG \equiv WG \equiv ncVEM

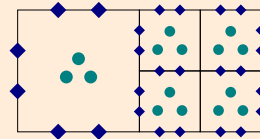
Cockburn, Di Pietro, Ern (2016)

Lemaire (2021)

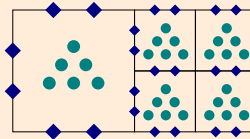
I.3. Further insight into HHO

- Local degrees of freedom:
 - Cell unknowns: $u_T \in P^{k'}(T)$
 - Face unknowns: $u_{\partial T} \in P^k(\partial T)$

EQUAL-ORDER: $k' = k$ ($= 1$)



MIXED-ORDER: $k' = k + 1$ ($= 2$)



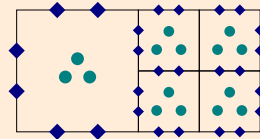
● CELL DOFS (DEGREE k')

◆ FACE DOFS (DEGREE k)

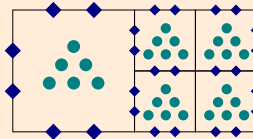
I.3. Further insight into HHO

- Local degrees of freedom:
 - Cell unknowns: $u_T \in P^{k'}(T)$
 - Face unknowns: $u_{\partial T} \in P^k(\partial T)$

EQUAL-ORDER: $k' = k$ ($= 1$)



MIXED-ORDER: $k' = k + 1$ ($= 2$)



● CELL DOFS (DEGREE k')

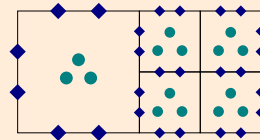
◆ FACE DOFS (DEGREE k)

Local HHO unknown: $\hat{u}_T := (\textcolor{teal}{u}_T, u_{\partial T}) \in \hat{P}_T^k := P^{k'}(T) \times P^k(\partial T)$

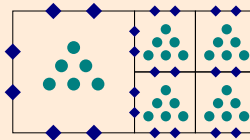
I.3. Further insight into HHO

- Local degrees of freedom:
 - Cell unknowns: $u_T \in P^{k'}(T)$
 - Face unknowns: $u_{\partial T} \in P^k(\partial T)$

EQUAL-ORDER: $k' = k$ ($= 1$)



MIXED-ORDER: $k' = k + 1$ ($= 2$)



● CELL DOFS (DEGREE k')

◆ FACE DOFS (DEGREE k)

Local HHO unknown: $\hat{u}_T := (\textcolor{teal}{u}_T, u_{\partial T}) \in \hat{P}_T^k := P^{k'}(T) \times P^k(\partial T)$

- Global degrees of freedom: $\hat{u}_{\mathcal{M}} := (\textcolor{teal}{u}_{\mathcal{T}}, u_{\mathcal{F}}) \in \hat{P}_{\mathcal{M}}^k := P_{\mathcal{T}}^{k'} \times P_{\mathcal{F}}^k$

► Cell unknowns: $u_{\mathcal{T}} \in P_{\mathcal{T}}^{k'} := \bigtimes_{T \in \mathcal{T}} P^{k'}(T)$

► Face unknowns: $u_{\mathcal{F}} \in P_{\mathcal{F}}^k := \bigtimes_{F \in \mathcal{F}} P^k(F)$

■ Algebraic realization for elliptic problem: $(\kappa \nabla u, \nabla w)_\Omega = (f, w)_\Omega$

$$\begin{bmatrix} \mathcal{K}_T & \mathcal{K}_{TF} \\ \mathcal{K}_{FT} & \mathcal{K}_F \end{bmatrix} \begin{bmatrix} U_T \\ U_F \end{bmatrix} = \begin{bmatrix} F_T \\ 0 \end{bmatrix}$$

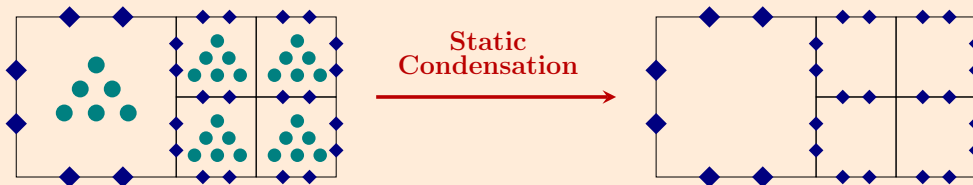
► Coupling between cell and face unknowns: $\mathcal{K}_F U_F = -\mathcal{K}_{FT} U_T$

- Algebraic realization for elliptic problem: $(\kappa \nabla u, \nabla w)_\Omega = (f, w)_\Omega$

$$\begin{bmatrix} \mathcal{K}_T & \mathcal{K}_{TF} \\ \mathcal{K}_{FT} & \mathcal{K}_F \end{bmatrix} \begin{bmatrix} U_T \\ U_F \end{bmatrix} = \begin{bmatrix} F_T \\ 0 \end{bmatrix}$$

- Coupling between cell and face unknowns: $\mathcal{K}_F U_F = -\mathcal{K}_{FT} U_T$

- Static condensation: Elimination of cell unknowns



■ Design of local operators

- **Gradient reconstruction** $(\nabla u)|_T \approx \mathbf{g}_T(\hat{u}_T) \in \mathbf{P}^k(T)$: design mimics **integration by parts**

$$\forall \hat{u}_T \in \widehat{P}_T^k \quad (\mathbf{g}_T(\hat{u}_T), \mathbf{q})_T = (\nabla u_T, \mathbf{q})_T - (u_T - u_{\partial T}, \mathbf{q} \cdot \mathbf{n}_T)_{\partial T}, \quad \forall \mathbf{q} \in \mathbf{P}^k(T)$$

■ Design of local operators

- **Gradient reconstruction** $(\nabla u)|_T \approx \mathbf{g}_T(\hat{u}_T) \in \mathbf{P}^k(T)$: design mimics **integration by parts**

$$\forall \hat{u}_T \in \widehat{P}_T^k \quad (\mathbf{g}_T(\hat{u}_T), \mathbf{q})_T = (\nabla u_T, \mathbf{q})_T - (u_T - u_{\partial T}, \mathbf{q} \cdot \mathbf{n}_T)_{\partial T}, \quad \forall \mathbf{q} \in \mathbf{P}^k(T)$$

- **Stabilization operator:** Weakly enforces matching of trace of cell dofs with face dofs

$$S_{\partial T}(\hat{u}_T) := \begin{cases} \Pi_{\partial T}^k(u_T|_{\partial T} - u_{\partial T}) & \text{mixed-order: Lehrenfeld–Schöberl (HDG)} \\ u_T|_{\partial T} - u_{\partial T} + \text{HOC} & \text{equal-order: High-order correction} \end{cases}$$

■ Design of local operators

- **Gradient reconstruction** $(\nabla u)|_T \approx \mathbf{g}_T(\hat{u}_T) \in \mathbf{P}^k(T)$: design mimics **integration by parts**

$$\forall \hat{u}_T \in \widehat{P}_T^k \quad (\mathbf{g}_T(\hat{u}_T), \mathbf{q})_T = (\nabla u_T, \mathbf{q})_T - (u_T - u_{\partial T}, \mathbf{q} \cdot \mathbf{n}_T)_{\partial T}, \quad \forall \mathbf{q} \in \mathbf{P}^k(T)$$

- **Stabilization operator:** Weakly enforces matching of trace of cell dofs with face dofs

$$S_{\partial T}(\hat{u}_T) := \begin{cases} \Pi_{\partial T}^k(u_T|_{\partial T} - u_{\partial T}) & \text{mixed-order: Lehrenfeld–Schöberl (HDG)} \\ u_T|_{\partial T} - u_{\partial T} + \text{HOC} & \text{equal-order: High-order correction} \end{cases}$$

■ Same advantages as dG with following improvements:

- ✓ Improved convergence rates: $\|\cdot\|_{H^1}$: $\mathcal{O}(h^{k+1})$ vs. $\mathcal{O}(h^k)$ & $\|\cdot\|_{L^2}$: $\mathcal{O}(h^{k+2})$ vs. $\mathcal{O}(h^{k+1})$
- ✓ Tuning-free and cell-based stabilization
- ✓ Attractive computational costs leveraging static condensation
- ✓ No integration needed on faces for nonlinear problems

Table of Contents

II - Elasto-acoustic coupling

II.1 Model problem

II.2 HHO space semi-discretization

II.3 Runge–Kutta time discretization

II.4 Numerical results



R. Mottier, A. Ern, R. Khot, L. Guillot (2025). Accepted to M2AN

Hybrid high-order methods for elasto-acoustic wave propagation in the time domain



R. Mottier, A. Ern, L. Guillot (2025). Submitted to CMAME

Elasto-acoustic wave propagation in geophysical media using hybrid high-order methods on general meshes

II.1. Model problem

- Wave equations in first-order formulation in time → **Wide range of efficient time integrators**

II.1. Model problem

- Wave equations in first-order formulation in time → Wide range of efficient time integrators

- ▶ Acoustic wave equation (in Ω^F):

$$\rho^F \partial_t \mathbf{v} - \nabla p = \mathbf{0}$$

$$\frac{1}{\kappa} \partial_t p - \nabla \cdot \mathbf{v} = \mathbf{f}^F$$

Unknowns: p pressure, \mathbf{v} velocity

Parameters: ρ^F , $\kappa \rightarrow c_p^F := \sqrt{\frac{\kappa}{\rho^F}}$

- ▶ Elastic wave equation (in Ω^S):

$$\mathbb{C}^{-1}(\lambda, \mu) \partial_t \mathbf{s} - \nabla_{\text{sym}} \mathbf{v} = \mathbf{0}$$

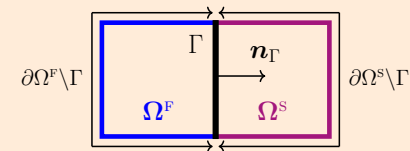
$$\rho^S \partial_t \mathbf{v} - \nabla \cdot \mathbf{s} = \mathbf{f}^S$$

Unknowns: \mathbf{v} velocity, \mathbf{s} stress

Parameters: ρ^S , $\mathbb{C} \rightarrow c_p^S := \sqrt{\frac{\lambda + 2\mu}{\rho^S}}$, $c_s := \sqrt{\frac{\mu}{\rho^S}}$

- Coupling conditions (on $\Gamma = \partial\Omega^F \cap \partial\Omega^S$):

- ▶ Kinematic condition: $\mathbf{v} \cdot \mathbf{n}_\Gamma = \mathbf{v} \cdot \mathbf{n}_\Gamma$
- ▶ Balance of forces per unit surface: $\mathbf{s} \cdot \mathbf{n}_\Gamma = p \mathbf{n}_\Gamma$



II.1. Model problem

- Wave equations in first-order formulation in time → Wide range of efficient time integrators

- Acoustic wave equation (in Ω^F):

$$\rho^F \partial_t \mathbf{v} - \nabla p = \mathbf{0}$$

$$\frac{1}{\kappa} \partial_t p - \nabla \cdot \mathbf{v} = \mathbf{f}^F$$

Unknowns: p pressure, \mathbf{v} velocity

Parameters: ρ^F , $\kappa \rightarrow c_p^F := \sqrt{\frac{\kappa}{\rho^F}}$

- Elastic wave equation (in Ω^S):

$$\mathbb{C}^{-1}(\lambda, \mu) \partial_t \mathbf{s} - \nabla_{\text{sym}} \mathbf{v} = \mathbf{0}$$

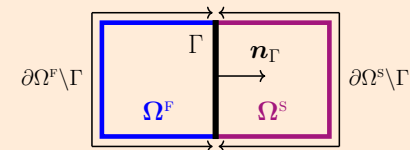
$$\rho^S \partial_t \mathbf{v} - \nabla \cdot \mathbf{s} = \mathbf{f}^S$$

Unknowns: \mathbf{v} velocity, \mathbf{s} stress

Parameters: ρ^S , $\mathbb{C} \rightarrow c_p^S := \sqrt{\frac{\lambda + 2\mu}{\rho^S}}$, $c_s := \sqrt{\frac{\mu}{\rho^S}}$

- Coupling conditions (on $\Gamma = \partial\Omega^F \cap \partial\Omega^S$):

- Kinematic condition: $\mathbf{v} \cdot \mathbf{n}_\Gamma = \mathbf{v} \cdot \mathbf{n}_\Gamma$
- Balance of forces per unit surface: $\mathbf{s} \cdot \mathbf{n}_\Gamma = p \mathbf{n}_\Gamma$



- Initial conditions on (p, \mathbf{v}) and (\mathbf{v}, \mathbf{s})

- Homogeneous Dirichlet boundary conditions on $\partial\Omega$ for simplicity

■ Approximation spaces

$$\begin{aligned} P^F &:= \{p \in H^1(\Omega^F) : p|_{\partial\Omega^F \setminus \Gamma} = 0\}, & M^F &:= L^2(\Omega^F) \\ V^S &:= \{v \in H^1(\Omega^S) : v|_{\partial\Omega^S \setminus \Gamma} = \mathbf{0}\}, & S^S &:= \mathbb{L}_{\text{sym}}^2(\Omega^S) \end{aligned}$$

■ Approximation spaces

$$\begin{aligned} P^F &:= \{p \in H^1(\Omega^F) : p|_{\partial\Omega^F \setminus \Gamma} = 0\}, & M^F &:= L^2(\Omega^F) \\ V^S &:= \{v \in H^1(\Omega^S) : v|_{\partial\Omega^S \setminus \Gamma} = 0\}, & S^S &:= \mathbb{L}_{\text{sym}}^2(\Omega^S) \end{aligned}$$

■ **Weak formulation:** Find $(v, p) : (0, T_f) \rightarrow M^F \times P^F$ and $(s, v) : (0, T_f) \rightarrow S^S \times V^S$ such that, $\forall t \in (0, T_f)$,

► **Acoustic wave equations:** $\forall (r, q) \in M^F \times P^F$,

$$(\partial_t v(t), r)_{\rho^F; \Omega^F} - (\nabla p(t), r)_{\Omega^F} = 0$$

$$(\partial_t p(t), q)_{\frac{1}{\kappa}; \Omega^F} + (v(t), \nabla q)_{\Omega^F} + (v(t) \cdot n_\Gamma, q)_\Gamma = (f^F(t), q)_{\Omega^F}$$

► **Elastic wave equations:** $\forall (b, w) \in S^S \times V^S$,

$$(\partial_t s(t), b)_{\mathbb{C}^{-1}; \Omega^S} - (\nabla_{\text{sym}} v(t), b)_{\Omega^S} = 0,$$

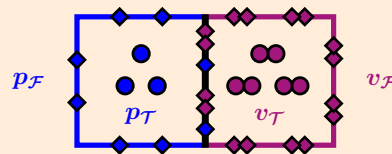
$$(\partial_t v(t), w)_{\rho^S; \Omega^S} + (s(t), \nabla_{\text{sym}} w)_{\Omega^S} - (p(t) n_\Gamma, w)_\Gamma = (f^S(t), w)_{\Omega^S}.$$

► **Skew-symmetry of differential operators**

► **Coupling conditions weakly imposed**

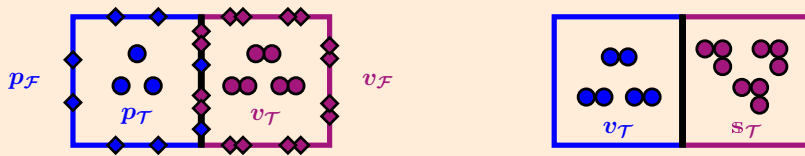
■ **Main idea:** Primal variables (\mathbf{p} , \mathbf{v}) \rightarrow HHO discretization

■ **Local dofs:** HHO: $\hat{\mathbf{p}}_T := (p_T, p_{\partial T}) \in \hat{P}_T^k$, $\hat{\mathbf{v}}_T := (v_T, v_{\partial T}) \in \hat{P}_T^k$



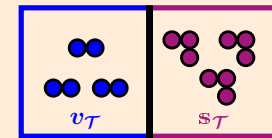
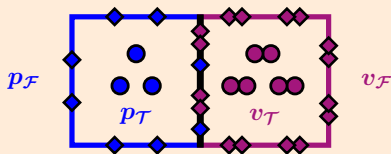
■ **Main idea:** Primal variables (p, v) → HHO discretization & Dual variables (v, s) → dG setting

■ **Local dofs:** HHO: $\hat{p}_T := (p_T, p_{\partial T}) \in \hat{P}_T^k$, $\hat{v}_T := (v_T, v_{\partial T}) \in \hat{P}_T^k$ dG: v_T, s_T



■ Main idea: Primal variables (\mathbf{p} , \mathbf{v}) → HHO discretization & Dual variables (\mathbf{v} , \mathbf{s}) → dG setting

■ Local dofs: HHO: $\hat{\mathbf{p}}_T := (p_T, p_{\partial T}) \in \hat{P}_T^k$, $\hat{\mathbf{v}}_T := (v_T, v_{\partial T}) \in \hat{P}_T^k$ dG: \mathbf{v}_T , \mathbf{s}_T



■ Global dofs: HHO: $\hat{\mathbf{p}}_{\mathcal{M}^F} := (p_{\mathcal{T}^F}, p_{\mathcal{F}^F}) \in \hat{P}_{\mathcal{M}^F}^k$, $\hat{\mathbf{v}}_{\mathcal{M}^S} := (v_{\mathcal{T}^S}, v_{\mathcal{F}^S}) \in \hat{P}_{\mathcal{M}^S}^k$ dG: $\mathbf{v}_{\mathcal{T}^F}$, $\mathbf{s}_{\mathcal{T}^S}$

$$p_{\mathcal{T}^F} \in P_{\mathcal{T}^F}^{k'} := \bigtimes_{T \in \mathcal{T}^F} P^{k'}(T), \quad p_{\mathcal{F}^F} \in P_{\mathcal{F}^F}^k := \bigtimes_{F \in \mathcal{F}^F} P^k(F), \quad \mathbf{v}_{\mathcal{T}^F} \in \mathbf{V}_{\mathcal{T}^F}^k := \bigtimes_{T \in \mathcal{T}^F} \mathbf{P}^k(T)$$

$$\mathbf{v}_{\mathcal{T}^S} \in \mathbf{V}_{\mathcal{T}^S}^{k'} := \bigtimes_{T \in \mathcal{T}^S} \mathbf{P}^{k'}(T), \quad \mathbf{v}_{\mathcal{F}^S} \in \mathbf{V}_{\mathcal{F}^S}^k := \bigtimes_{F \in \mathcal{F}^S} \mathbf{P}^k(F), \quad \mathbf{s}_{\mathcal{T}^S} \in \mathbb{S}_{\mathcal{T}^S}^k := \bigtimes_{T \in \mathcal{T}^S} \mathbb{P}_{\text{sym}}^k(T)$$

II.2. HHO space semi-discretization

- **Acoustic weak formulation (recall):** Find $(\mathbf{v}, p) : (0, T_f) \rightarrow \mathbf{M}^F \times P^F$ such that, $\forall t \in (0, T_f)$,

$$(\partial_t \mathbf{v}(t), \mathbf{r})_{(\rho^F; \Omega^F)} - (\nabla p(t), \mathbf{r})_{\Omega^F} = 0$$

$$(\partial_t p(t), q)_{(\frac{1}{\kappa}; \Omega^F)} + (\mathbf{v}(t), \nabla q)_{\Omega^F} + (\mathbf{v}(t) \cdot \mathbf{n}_\Gamma, q)_\Gamma = (f^F(t), q)_{\Omega^F}$$

- **Acoustic wave equation:** Find $(\hat{p}_{\mathcal{M}^F}, \mathbf{v}_{\mathcal{T}^F}) : (0, T_f) \longrightarrow \hat{P}_{\mathcal{M}^F}^k \times \mathbf{V}_{\mathcal{T}^F}^k$ such that, $\forall t \in (0, T_f)$,

$$(\partial_t \mathbf{v}_{\mathcal{T}^F}(t), \mathbf{r}_{\mathcal{T}^F})_{(\rho^F; \Omega^F)} - (\mathbf{g}_{\mathcal{T}^F}(\hat{p}_{\mathcal{M}^F}(t)), \mathbf{r}_{\mathcal{T}^F})_{\Omega^F} = 0$$

$$(\partial_t p_{\mathcal{T}^F}(t), q_{\mathcal{T}^F})_{(\frac{1}{\kappa}; \Omega^F)} + (\mathbf{v}_{\mathcal{T}^F}(t), \mathbf{g}_{\mathcal{T}^F}(\hat{q}_{\mathcal{M}^F}))_{\Omega^F} + s_{\mathcal{M}^F}(\hat{p}_{\mathcal{M}^F}(t), \hat{q}_{\mathcal{M}^F}) + (\mathbf{v}_{\mathcal{F}^S}(t) \cdot \mathbf{n}_\Gamma, q_{\mathcal{F}^F})_\Gamma = (f^F(t), q_{\mathcal{T}^F})_{\Omega^F}$$

II.2. HHO space semi-discretization

- **Acoustic weak formulation (recall):** Find $(\mathbf{v}, p) : (0, T_f) \rightarrow \mathbf{M}^F \times P^F$ such that, $\forall t \in (0, T_f)$,

$$(\partial_t \mathbf{v}(t), \mathbf{r})_{(\rho^F; \Omega^F)} - (\nabla p(t), \mathbf{r})_{\Omega^F} = 0$$

$$(\partial_t p(t), q)_{(\frac{1}{\kappa}; \Omega^F)} + (\mathbf{v}(t), \nabla q)_{\Omega^F} + (\mathbf{v}(t) \cdot \mathbf{n}_\Gamma, q)_\Gamma = (f^F(t), q)_{\Omega^F}$$

- **Acoustic wave equation:** Find $(\hat{p}_{\mathcal{M}^F}, \mathbf{v}_{\mathcal{T}^F}) : (0, T_f) \rightarrow \hat{P}_{\mathcal{M}^F}^k \times \mathbf{V}_{\mathcal{T}^F}^k$ such that, $\forall t \in (0, T_f)$,

$$(\partial_t \mathbf{v}_{\mathcal{T}^F}(t), \mathbf{r}_{\mathcal{T}^F})_{(\rho^F; \Omega^F)} - (\mathbf{g}_{\mathcal{T}^F}(\hat{p}_{\mathcal{M}^F}(t)), \mathbf{r}_{\mathcal{T}^F})_{\Omega^F} = 0$$

$$(\partial_t p_{\mathcal{T}^F}(t), q_{\mathcal{T}^F})_{(\frac{1}{\kappa}; \Omega^F)} + (\mathbf{v}_{\mathcal{T}^F}(t), \mathbf{g}_{\mathcal{T}^F}(\hat{q}_{\mathcal{M}^F}))_{\Omega^F} + s_{\mathcal{M}^F}(\hat{p}_{\mathcal{M}^F}(t), \hat{q}_{\mathcal{M}^F}) + (\mathbf{v}_{\mathcal{F}^S}(t) \cdot \mathbf{n}_\Gamma, q_{\mathcal{F}^F})_\Gamma = (f^F(t), q_{\mathcal{T}^F})_{\Omega^F}$$

- **Elastic wave equation:** Find $(\hat{\mathbf{v}}_{\mathcal{M}^S}, \mathbf{s}_{\mathcal{T}^S}) : (0, T_f) \rightarrow \hat{\mathbf{V}}_{\mathcal{M}^S}^k \times \mathbb{S}_{\mathcal{T}^S}^k$ such that, $\forall t \in (0, T_f)$,

$$(\partial_t \mathbf{s}_{\mathcal{T}^S}(t), \mathbf{b}_{\mathcal{T}^S})_{(\mathbb{C}^{-1}; \Omega^S)} - (\mathbf{g}_{\mathcal{T}^S}^{\text{sym}}(\hat{\mathbf{v}}_{\mathcal{M}^S}(t)), \mathbf{b}_{\mathcal{T}^S})_{\Omega^S} = 0$$

$$(\partial_t \mathbf{v}_{\mathcal{T}^S}(t), \mathbf{w}_{\mathcal{T}^S})_{(\rho^S; \Omega^S)} + (\mathbf{s}_{\mathcal{T}^S}(t), \mathbf{g}_{\mathcal{T}^S}^{\text{sym}}(\hat{\mathbf{w}}_{\mathcal{M}^S}))_{\Omega^S} + s_{\mathcal{M}^S}(\hat{\mathbf{v}}_{\mathcal{M}^S}(t), \hat{\mathbf{w}}_{\mathcal{M}^S}) - (p_{\mathcal{F}^F}(t) \mathbf{n}_\Gamma, \mathbf{w}_{\mathcal{F}^S})_\Gamma = (\mathbf{f}^S(t), \mathbf{w}_{\mathcal{T}^S})_{\Omega^S}$$

II.2. HHO space semi-discretization

- **Acoustic weak formulation (recall):** Find $(\mathbf{v}, p) : (0, T_f) \rightarrow \mathbf{M}^F \times P^F$ such that, $\forall t \in (0, T_f)$,

$$(\partial_t \mathbf{v}(t), \mathbf{r})_{(\rho^F; \Omega^F)} - (\nabla p(t), \mathbf{r})_{\Omega^F} = 0$$

$$(\partial_t p(t), q)_{(\frac{1}{\kappa}; \Omega^F)} + (\mathbf{v}(t), \nabla q)_{\Omega^F} + (\mathbf{v}(t) \cdot \mathbf{n}_\Gamma, q)_\Gamma = (f^F(t), q)_{\Omega^F}$$

- **Acoustic wave equation:** Find $(\hat{p}_{\mathcal{M}^F}, \mathbf{v}_{\mathcal{T}^F}) : (0, T_f) \rightarrow \hat{P}_{\mathcal{M}^F}^k \times \mathbf{V}_{\mathcal{T}^F}^k$ such that, $\forall t \in (0, T_f)$,

$$(\partial_t \mathbf{v}_{\mathcal{T}^F}(t), \mathbf{r}_{\mathcal{T}^F})_{(\rho^F; \Omega^F)} - (\mathbf{g}_{\mathcal{T}^F}(\hat{p}_{\mathcal{M}^F}(t)), \mathbf{r}_{\mathcal{T}^F})_{\Omega^F} = 0$$

$$(\partial_t p_{\mathcal{T}^F}(t), q_{\mathcal{T}^F})_{(\frac{1}{\kappa}; \Omega^F)} + (\mathbf{v}_{\mathcal{T}^F}(t), \mathbf{g}_{\mathcal{T}^F}(\hat{q}_{\mathcal{M}^F}))_{\Omega^F} + s_{\mathcal{M}^F}(\hat{p}_{\mathcal{M}^F}(t), \hat{q}_{\mathcal{M}^F}) + (\mathbf{v}_{\mathcal{F}^S}(t) \cdot \mathbf{n}_\Gamma, q_{\mathcal{F}^F})_\Gamma = (f^F(t), q_{\mathcal{T}^F})_{\Omega^F}$$

- **Elastic wave equation:** Find $(\hat{\mathbf{v}}_{\mathcal{M}^S}, \mathbf{s}_{\mathcal{T}^S}) : (0, T_f) \rightarrow \hat{\mathbf{V}}_{\mathcal{M}^S}^k \times \mathbb{S}_{\mathcal{T}^S}^k$ such that, $\forall t \in (0, T_f)$,

$$(\partial_t \mathbf{s}_{\mathcal{T}^S}(t), \mathbf{b}_{\mathcal{T}^S})_{(\mathbb{C}^{-1}; \Omega^S)} - (\mathbf{g}_{\mathcal{T}^S}^{\text{sym}}(\hat{\mathbf{v}}_{\mathcal{M}^S}(t)), \mathbf{b}_{\mathcal{T}^S})_{\Omega^S} = 0$$

$$(\partial_t \mathbf{v}_{\mathcal{T}^S}(t), \mathbf{w}_{\mathcal{T}^S})_{(\rho^S; \Omega^S)} + (\mathbf{s}_{\mathcal{T}^S}(t), \mathbf{g}_{\mathcal{T}^S}^{\text{sym}}(\hat{\mathbf{w}}_{\mathcal{M}^S}))_{\Omega^S} + s_{\mathcal{M}^S}(\hat{\mathbf{v}}_{\mathcal{M}^S}(t), \hat{\mathbf{w}}_{\mathcal{M}^S}) - (p_{\mathcal{F}^F}(t) \mathbf{n}_\Gamma, \mathbf{w}_{\mathcal{F}^S})_\Gamma = (\mathbf{f}^S(t), \mathbf{w}_{\mathcal{T}^S})_{\Omega^S}$$

- **Stabilizations act only on primal variables**

■ Global stabilization:

- ▶ $s_{\mathcal{M}^F}(\hat{p}_{\mathcal{M}^F}, \hat{q}_{\mathcal{M}^F}) := \sum_{T \in \mathcal{T}^F} \tau_T^F(S_{\partial T}(\hat{p}_T), S_{\partial T}(\hat{q}_T))_{\partial T}$
- ▶ $s_{\mathcal{M}^S}(\hat{\mathbf{v}}_{\mathcal{M}^S}, \hat{\mathbf{w}}_{\mathcal{M}^S}) := \sum_{T \in \mathcal{T}^S} \tau_T^S(\mathbf{S}_{\partial T}(\hat{\mathbf{v}}_T), \mathbf{S}_{\partial T}(\hat{\mathbf{w}}_T))_{\partial T}$

■ Global stabilization:

- $s_{\mathcal{M}^F}(\hat{p}_{\mathcal{M}^F}, \hat{q}_{\mathcal{M}^F}) := \sum_{T \in \mathcal{T}^F} \tau_T^F(S_{\partial T}(\hat{p}_T), S_{\partial T}(\hat{q}_T))_{\partial T}$
 - $s_{\mathcal{M}^S}(\hat{v}_{\mathcal{M}^S}, \hat{w}_{\mathcal{M}^S}) := \sum_{T \in \mathcal{T}^S} \tau_T^S(S_{\partial T}(\hat{v}_T), S_{\partial T}(\hat{w}_T))_{\partial T}$

Two strategies:

$$\tau_T^S = \mathcal{O}(\frac{1}{h}) = \tau_T^F$$

(standard for elliptic problem)

on

$$\tau_T^S = \mathcal{O}(1) = \tau_T^F$$

(standard for hyperbolic problem)

■ Global stabilization:

- $s_{\mathcal{M}^F}(\hat{p}_{\mathcal{M}^F}, \hat{q}_{\mathcal{M}^F}) := \sum_{T \in \mathcal{T}^F} \tau_T^F(S_{\partial T}(\hat{p}_T), S_{\partial T}(\hat{q}_T))_{\partial T}$
- $s_{\mathcal{M}^S}(\hat{\mathbf{v}}_{\mathcal{M}^S}, \hat{\mathbf{w}}_{\mathcal{M}^S}) := \sum_{T \in \mathcal{T}^S} \tau_T^S(S_{\partial T}(\hat{\mathbf{v}}_T), S_{\partial T}(\hat{\mathbf{w}}_T))_{\partial T}$

Two strategies:

■ **Mechanical energy:** $\mathcal{E}_h(t) := \frac{1}{2} \|\boldsymbol{v}_{\mathcal{T}}(t)\|_{\rho^F; \Omega^F}^2 + \frac{1}{2} \|p_{\mathcal{T}}(t)\|_{\frac{1}{\kappa}; \Omega^F}^2 + \frac{1}{2} \|\boldsymbol{v}_{\mathcal{T}}(t)\|_{\rho^S; \Omega^S}^2 + \frac{1}{2} \|\boldsymbol{s}_{\mathcal{T}}(t)\|_{\mathbb{C}^{-1}; \Omega^S}^2$

■ Space semi-discrete energy balance

$$\mathcal{E}_h(t) + \int_0^t \left\{ s_{\mathcal{M}^F}(\hat{p}_{\mathcal{M}^F}(\tau), \hat{p}_{\mathcal{M}^F}(\tau)) + s_{\mathcal{M}^S}(\hat{\mathbf{v}}_{\mathcal{M}^S}(\tau), \hat{\mathbf{v}}_{\mathcal{M}^S}(\tau)) \right\} d\tau = \\ \mathcal{E}_h(0) + \int_0^t \left\{ (f^F(\tau), \mathbf{p}_{\mathcal{T}^F}(\tau))_{\Omega^F} + (\mathbf{f}^S(\tau), \mathbf{v}_{\mathcal{T}^S}(\tau))_{\Omega^S} \right\} d\tau$$

■ Error analysis (under maximal regularity assumption)

$$\begin{aligned} \|\mathbf{v} - \mathbf{v}_{\mathcal{T}^F}\|_{\rho^F; \Omega^F} + \|p - p_{\mathcal{T}^F}\|_{\frac{1}{\kappa}; \Omega^F} &\lesssim \begin{cases} \mathcal{O}(h^{k+\frac{1}{2}}) & \text{for } \mathcal{O}(1)\text{-stabilization} \\ \mathcal{O}(h^{k+1}) & \text{for } \mathcal{O}(\frac{1}{h})\text{-stabilization \& } k' = k + 1 \end{cases} \\ + \|\mathbf{s} - \mathbf{s}_{\mathcal{T}^S}\|_{\mathbb{C}^{-1}; \Omega^S} + \|\mathbf{v} - \mathbf{v}_{\mathcal{T}^S}\|_{\rho^S; \Omega^S} \end{aligned}$$

■ Error analysis (under maximal regularity assumption)

$$\begin{aligned} \|\mathbf{v} - \mathbf{v}_{\mathcal{T}^F}\|_{\rho^F; \Omega^F} + \|p - p_{\mathcal{T}^F}\|_{\frac{1}{\kappa}; \Omega^F} &\lesssim \begin{cases} \mathcal{O}(h^{k+\frac{1}{2}}) & \text{for } \mathcal{O}(1)\text{-stabilization} \\ \mathcal{O}(h^{k+1}) & \text{for } \mathcal{O}(\frac{1}{h})\text{-stabilization \& } k' = k + 1 \end{cases} \\ + \|\mathbf{s} - \mathbf{s}_{\mathcal{T}^S}\|_{\mathbb{C}^{-1}; \Omega^S} + \|\mathbf{v} - \mathbf{v}_{\mathcal{T}^S}\|_{\rho^S; \Omega^S} \end{aligned}$$

■ Key arguments

- ▶ L^2 -projection for HHO unknowns and HDG⁺-projection for dG unknowns  [Du, Sayas \(2019\)](#)
- ▶ **Error Equations:** Difference between projected exact solution and scheme equations
- ▶ **Stability:** Testing with discrete errors + using classical inequalities
→ discrete energy on lhs and consistency error on rhs
- ▶ **Consistency error bound**

■ Use of the HDG-projection [Cockburn, Gopalakrishnan, Sayas \(2010\)](#)

■ On simplices with $\mathcal{O}(1)$ -stabilization [Ern, Khot \(2024+\):](#)

$$k + \frac{1}{2} \longrightarrow k + 1$$

■ Space semi-discrete algebraic realization

$$\left[\begin{array}{ccc|cc} \mathcal{M}_{\mathcal{T}^F}^{\rho^F} & 0 & 0 & 0 & 0 \\ 0 & \mathcal{M}_{\mathcal{T}^F}^{\frac{1}{\kappa}} & 0 & 0 & 0 \\ 0 & 0 & \mathcal{M}_{\mathcal{T}^S}^{C^{-1}} & 0 & 0 \\ 0 & 0 & 0 & \mathcal{M}_{\mathcal{T}^S}^{\rho^S} & 0 \\ \hline 0 & 0 & 0 & 0 & 0 \\ 0 & 0 & 0 & 0 & 0 \end{array} \right] \frac{d}{dt} \begin{bmatrix} \mathbf{M}_{\mathcal{T}^F} \\ \mathbf{P}_{\mathcal{T}^F} \\ \mathbf{S}_{\mathcal{T}^S} \\ \mathbf{V}_{\mathcal{T}^S} \\ \hline \mathbf{P}_{\mathcal{F}^F} \\ \mathbf{V}_{\mathcal{F}^S} \end{bmatrix} + \begin{bmatrix} 0 & \mathcal{G}_{\mathcal{T}^F} & 0 & 0 & \mathcal{G}_{\mathcal{T}^F \mathcal{F}^F} & 0 \\ -\mathcal{G}_{\mathcal{T}^F}^\dagger & \Sigma_{\mathcal{T}^F} & 0 & 0 & \Sigma_{\mathcal{T}^F \mathcal{F}^F} & 0 \\ 0 & 0 & 0 & \mathcal{H}_{\mathcal{T}^S} & 0 & \mathcal{H}_{\mathcal{T}^S \mathcal{F}^S} \\ 0 & 0 & -\mathcal{H}_{\mathcal{T}^S}^\dagger & \Sigma_{\mathcal{T}^S} & 0 & \Sigma_{\mathcal{T}^S \mathcal{F}^S} \\ \hline -\mathcal{G}_{\mathcal{T}^F \mathcal{F}^F}^\dagger & \Sigma_{\mathcal{T}^F \mathcal{F}^F}^\dagger & 0 & 0 & \Sigma_{\mathcal{F}^F} & \mathcal{C}_{\mathcal{F}^F} \\ 0 & 0 & -\mathcal{H}_{\mathcal{T}^S \mathcal{F}^S}^\dagger & \Sigma_{\mathcal{T}^S \mathcal{F}^S}^\dagger & -\mathcal{C}_{\mathcal{F}^F}^\dagger & \Sigma_{\mathcal{F}^S} \end{bmatrix} \begin{bmatrix} \mathbf{M}_{\mathcal{T}^F} \\ \mathbf{P}_{\mathcal{T}^F} \\ \mathbf{S}_{\mathcal{T}^S} \\ \mathbf{V}_{\mathcal{T}^S} \\ \hline \mathbf{P}_{\mathcal{F}^F} \\ \mathbf{V}_{\mathcal{F}^S} \end{bmatrix} = \begin{bmatrix} 0 \\ \mathbf{F}_{\mathcal{T}^F} \\ 0 \\ \mathbf{F}_{\mathcal{T}^S} \\ 0 \\ 0 \end{bmatrix}$$

■ Space semi-discrete algebraic realization

$$\left[\begin{array}{ccc|cc} \mathcal{M}_{\mathcal{T}^F}^{\rho^F} & 0 & 0 & 0 & 0 \\ 0 & \mathcal{M}_{\mathcal{T}^F}^{\frac{1}{\kappa}} & 0 & 0 & 0 \\ 0 & 0 & \mathcal{M}_{\mathcal{T}^S}^{C^{-1}} & 0 & 0 \\ 0 & 0 & 0 & \mathcal{M}_{\mathcal{T}^S}^{\rho^S} & 0 \\ \hline 0 & 0 & 0 & 0 & 0 \\ 0 & 0 & 0 & 0 & 0 \end{array} \right] \frac{d}{dt} \begin{bmatrix} \mathbf{M}_{\mathcal{T}^F} \\ \mathbf{P}_{\mathcal{T}^F} \\ \mathbf{S}_{\mathcal{T}^S} \\ \mathbf{V}_{\mathcal{T}^S} \\ \hline \mathbf{P}_{\mathcal{F}^F} \\ \mathbf{V}_{\mathcal{F}^S} \end{bmatrix} + \begin{bmatrix} 0 & \mathcal{G}_{\mathcal{T}^F} & 0 & 0 & \mathcal{G}_{\mathcal{T}^F \mathcal{F}^F} & 0 \\ -\mathcal{G}_{\mathcal{T}^F}^\dagger & \Sigma_{\mathcal{T}^F} & 0 & 0 & \Sigma_{\mathcal{T}^F \mathcal{F}^F} & 0 \\ 0 & 0 & 0 & \mathcal{H}_{\mathcal{T}^S} & 0 & \mathcal{H}_{\mathcal{T}^S \mathcal{F}^S} \\ 0 & 0 & -\mathcal{H}_{\mathcal{T}^S}^\dagger & \Sigma_{\mathcal{T}^S} & 0 & \Sigma_{\mathcal{T}^S \mathcal{F}^S} \\ \hline -\mathcal{G}_{\mathcal{T}^F \mathcal{F}^F}^\dagger & \Sigma_{\mathcal{T}^F \mathcal{F}^F}^\dagger & 0 & 0 & \Sigma_{\mathcal{F}^F} & \mathcal{C}_{\mathcal{F}^F} \\ 0 & 0 & -\mathcal{H}_{\mathcal{T}^S \mathcal{F}^S}^\dagger & \Sigma_{\mathcal{T}^S \mathcal{F}^S}^\dagger & -\mathcal{C}_{\mathcal{F}^F}^\dagger & \Sigma_{\mathcal{F}^S} \end{bmatrix} \begin{bmatrix} \mathbf{M}_{\mathcal{T}^F} \\ \mathbf{P}_{\mathcal{T}^F} \\ \mathbf{S}_{\mathcal{T}^S} \\ \mathbf{V}_{\mathcal{T}^S} \\ \hline \mathbf{P}_{\mathcal{F}^F} \\ \mathbf{V}_{\mathcal{F}^S} \end{bmatrix} = \begin{bmatrix} 0 \\ \mathbf{F}_{\mathcal{T}^F} \\ 0 \\ \mathbf{F}_{\mathcal{T}^S} \\ \hline 0 \\ 0 \end{bmatrix}$$

■ Compact formulation:

$$\begin{bmatrix} \mathcal{M}_{\mathcal{T}} & 0 \\ 0 & 0 \end{bmatrix} \frac{d}{dt} \begin{bmatrix} \mathbf{U}_{\mathcal{T}} \\ \mathbf{U}_{\mathcal{F}} \end{bmatrix} + \begin{bmatrix} \mathcal{K}_{\mathcal{T}} & \mathcal{K}_{\mathcal{T} \mathcal{F}} \\ \mathcal{K}_{\mathcal{F} \mathcal{T}} & \mathcal{K}_{\mathcal{F}} \end{bmatrix} \begin{bmatrix} \mathbf{U}_{\mathcal{T}} \\ \mathbf{U}_{\mathcal{F}} \end{bmatrix} = \begin{bmatrix} \mathbf{F}_{\mathcal{T}} \\ 0 \end{bmatrix}$$

■ Space semi-discrete algebraic realization

$$\left[\begin{array}{ccc|cc} M_{\mathcal{T}^F}^{\rho^F} & 0 & 0 & 0 & 0 \\ 0 & M_{\mathcal{T}^F}^{\frac{1}{\kappa}} & 0 & 0 & 0 \\ 0 & 0 & M_{\mathcal{T}^S}^{C^{-1}} & 0 & 0 \\ 0 & 0 & 0 & M_{\mathcal{T}^S}^{\rho^S} & 0 \\ \hline 0 & 0 & 0 & 0 & 0 \\ 0 & 0 & 0 & 0 & 0 \\ 0 & 0 & 0 & 0 & 0 \end{array} \right] \frac{d}{dt} \left[\begin{array}{c} M_{\mathcal{T}^F} \\ P_{\mathcal{T}^F} \\ S_{\mathcal{T}^S} \\ V_{\mathcal{T}^S} \\ \hline P_{\mathcal{F}^F} \\ V_{\mathcal{F}^S} \end{array} \right] + \left[\begin{array}{ccccc|cc} 0 & G_{\mathcal{T}^F} & 0 & 0 & G_{\mathcal{T}^F \mathcal{F}^F} & 0 \\ -G_{\mathcal{T}^F}^\dagger & \Sigma_{\mathcal{T}^F} & 0 & 0 & \Sigma_{\mathcal{T}^F \mathcal{F}^F} & 0 \\ 0 & 0 & 0 & \mathcal{H}_{\mathcal{T}^S} & 0 & \mathcal{H}_{\mathcal{T}^S \mathcal{F}^S} \\ 0 & 0 & -\mathcal{H}_{\mathcal{T}^S}^\dagger & \Sigma_{\mathcal{T}^S} & 0 & \Sigma_{\mathcal{T}^S \mathcal{F}^S} \\ \hline -G_{\mathcal{T}^F \mathcal{F}^F}^\dagger & \Sigma_{\mathcal{T}^F \mathcal{F}^F}^\dagger & 0 & 0 & \Sigma_{\mathcal{F}^F} & \mathcal{C}_{\mathcal{F}^F} \\ 0 & 0 & -\mathcal{H}_{\mathcal{T}^S \mathcal{F}^S}^\dagger & \Sigma_{\mathcal{T}^S \mathcal{F}^S}^\dagger & -\mathcal{C}_{\mathcal{F}^F}^\dagger & \Sigma_{\mathcal{F}^S} \end{array} \right] \left[\begin{array}{c} M_{\mathcal{T}^F} \\ P_{\mathcal{T}^F} \\ S_{\mathcal{T}^S} \\ V_{\mathcal{T}^S} \\ \hline P_{\mathcal{F}^F} \\ V_{\mathcal{F}^S} \end{array} \right] = \left[\begin{array}{c} 0 \\ F_{\mathcal{T}^F} \\ 0 \\ F_{\mathcal{T}^S} \\ 0 \\ 0 \end{array} \right]$$

■ Compact formulation:

$$\left[\begin{array}{cc} M_{\mathcal{T}} & 0 \\ 0 & 0 \end{array} \right] \frac{d}{dt} \left[\begin{array}{c} U_{\mathcal{T}} \\ U_{\mathcal{F}} \end{array} \right] + \left[\begin{array}{cc} \mathcal{K}_{\mathcal{T}} & \mathcal{K}_{\mathcal{T} \mathcal{F}} \\ \mathcal{K}_{\mathcal{F} \mathcal{T}} & \mathcal{K}_{\mathcal{F}} \end{array} \right] \left[\begin{array}{c} U_{\mathcal{T}} \\ U_{\mathcal{F}} \end{array} \right] = \left[\begin{array}{c} F_{\mathcal{T}} \\ 0 \end{array} \right]$$

- ▶ $\mathcal{K}_{\mathcal{T}}$ is trivially block-diagonal
- ▶ Key question: Is $\mathcal{K}_{\mathcal{F}}$ block-diagonal ? (Important for explicit schemes)

■ Structure of $\mathcal{K}_{\mathcal{F}}$:

$$\mathcal{K}_{\mathcal{F}} = \begin{bmatrix} \Sigma_{\mathcal{F}^{\text{OF}}} & \mathcal{C}_{\mathcal{F}^{\Gamma}} \\ -\mathcal{C}_{\mathcal{F}^{\Gamma}} & \Sigma_{\mathcal{F}^{\text{OS}}} \end{bmatrix} = \begin{bmatrix} \Sigma_{\mathcal{F}^{\text{OF}}} & 0 & 0 & 0 \\ 0 & \Sigma_{\mathcal{F}^{\text{OS}}} & 0 & 0 \\ 0 & 0 & \Sigma_{\mathcal{F}^{\Gamma}} & \mathcal{C}_{\mathcal{F}^{\Gamma}} \\ 0 & 0 & -\mathcal{C}_{\mathcal{F}^{\Gamma}} & \Sigma_{\mathcal{F}^{\Gamma}} \end{bmatrix}$$

■ Structure of $\mathcal{K}_{\mathcal{F}}$:

$$\mathcal{K}_{\mathcal{F}} = \begin{bmatrix} \Sigma_{\mathcal{F}^{\text{OF}}} & \mathcal{C}_{\mathcal{F}^{\Gamma}} \\ -\mathcal{C}_{\mathcal{F}^{\Gamma}} & \Sigma_{\mathcal{F}^{\text{S}}} \end{bmatrix} = \begin{bmatrix} \Sigma_{\mathcal{F}^{\text{OF}}} & 0 & 0 & 0 \\ 0 & \Sigma_{\mathcal{F}^{\text{OS}}} & 0 & 0 \\ 0 & 0 & \Sigma_{\mathcal{F}^{\Gamma}} & \mathcal{C}_{\mathcal{F}^{\Gamma}} \\ 0 & 0 & -\mathcal{C}_{\mathcal{F}^{\Gamma}} & \Sigma_{\mathcal{F}^{\Gamma}} \end{bmatrix}$$

- $\Sigma_{\mathcal{F}^{\text{F}}}$ and $\Sigma_{\mathcal{F}^{\text{S}}}$ block-diagonal only for **Lehrenfeld–Schöberl** and **Least-squares** stabilizations

$$S_{\partial T}(\hat{p}_T) := \begin{cases} \Pi_{\partial T}^k(p_T|_{\partial T} - p_{\partial T}) & \text{mixed-order: Lehrenfeld–Schöberl (HDG)} \\ p_T|_{\partial T} - p_{\partial T} + \text{H}\times\text{C} & \text{equal-order: Plain Least-squares} \end{cases}$$

■ Structure of $\mathcal{K}_{\mathcal{F}}$:

$$\mathcal{K}_{\mathcal{F}} = \begin{bmatrix} \Sigma_{\mathcal{F}^F} & \mathcal{C}_{\mathcal{F}^G} \\ -\mathcal{C}_{\mathcal{F}^G} & \Sigma_{\mathcal{F}^S} \end{bmatrix} = \begin{bmatrix} \Sigma_{\mathcal{F}^{OF}} & 0 & 0 & 0 \\ 0 & \Sigma_{\mathcal{F}^{OS}} & 0 & 0 \\ 0 & 0 & \boxed{\begin{matrix} \Sigma_{\mathcal{F}^G} & \mathcal{C}_{\mathcal{F}^G} \\ -\mathcal{C}_{\mathcal{F}^G} & \Sigma_{\mathcal{F}^G} \end{matrix}} \\ 0 & 0 & -\mathcal{C}_{\mathcal{F}^G} & \Sigma_{\mathcal{F}^G} \end{bmatrix} \quad \begin{bmatrix} \Sigma_{F_1^G} & \mathcal{C}_{F_1^G} & 0 & 0 & 0 \\ -\mathcal{C}_{F_1^G} & \Sigma_{F_1^G} & 0 & \vdots & \vdots \\ \vdots & \vdots & 0 & 0 & 0 \\ 0 & 0 & \ddots & 0 & 0 \\ 0 & 0 & 0 & \Sigma_{F_n^G} & \mathcal{C}_{F_1^G} \\ 0 & 0 & 0 & -\mathcal{C}_{F_n^G} & \Sigma_{F_n^G} \end{bmatrix}$$

- $\Sigma_{\mathcal{F}^F}$ and $\Sigma_{\mathcal{F}^S}$ block-diagonal only for **Lehrenfeld–Schöberl** and **Least-squares** stabilizations

$$S_{\partial T}(\hat{p}_T) := \begin{cases} \Pi_{\partial T}^k(p_T|_{\partial T} - p_{\partial T}) & \text{mixed-order: Lehrenfeld–Schöberl (HDG)} \\ p_T|_{\partial T} - p_{\partial T} + \text{H}\times\text{C} & \text{equal-order: Plain Least-squares} \end{cases}$$

- **Coupling terms at interface:** grouping acoustic and elastic dofs of each face

→ $\mathcal{K}_{\mathcal{F}}$ is block diagonal

II.3. Runge-Kutta time discretization

- Recall

$$\begin{bmatrix} \mathcal{M}_T & 0 \\ 0 & 0 \end{bmatrix} \frac{d}{dt} \begin{bmatrix} \mathbf{U}_T \\ \mathbf{U}_{\mathcal{F}} \end{bmatrix} + \begin{bmatrix} \mathcal{K}_T & \mathcal{K}_{T\mathcal{F}} \\ \mathcal{K}_{\mathcal{F}T} & \mathcal{K}_{\mathcal{F}} \end{bmatrix} \begin{bmatrix} \mathbf{U}_T \\ \mathbf{U}_{\mathcal{F}} \end{bmatrix} = \begin{bmatrix} \mathbf{F}_T \\ 0 \end{bmatrix}$$

s-stage Runge-Kutta schemes

SDIRK($s, s+1$) : Truncation order: $\mathcal{O}(\Delta t^{s+1})$

c_1	a_*	0	\dots	0	
c_2	a_{21}	a_*	\ddots	0	
\vdots	\vdots	\ddots	\ddots	\vdots	
c_s	a_{s1}	\dots	$a_{s,s-1}$	a_*	

ERK(s) : Truncation order: $\mathcal{O}(\Delta t^s)$

c_1	0	\dots	\dots	0	
c_2	a_{21}	0	\dots	0	
\vdots	\vdots	\ddots	\ddots	\vdots	
c_s	a_{s1}	\dots	$a_{s,s-1}$	0	

■ **SDIRK($s, s+1$) schemes:** For all $i \in \{1, \dots, s\}$,

$$\begin{bmatrix} \mathcal{M}_{\mathcal{T}} & 0 \\ 0 & 0 \end{bmatrix} \begin{bmatrix} \mathbf{U}_{\mathcal{T}}^{n,i} \\ \mathbf{U}_{\mathcal{F}}^{n,i} \end{bmatrix} = \begin{bmatrix} \mathcal{M}_{\mathcal{T}} & 0 \\ 0 & 0 \end{bmatrix} \begin{bmatrix} \mathbf{U}_{\mathcal{T}}^{n-1} \\ \mathbf{U}_{\mathcal{F}}^{n-1} \end{bmatrix} + \Delta t \sum_{j=1}^{\textcolor{red}{i}} a_{ij} \left(\begin{bmatrix} \mathbf{F}_{\mathcal{T}}^{n-1+c_j} \\ 0 \end{bmatrix} - \begin{bmatrix} \mathcal{K}_{\mathcal{T}} & \mathcal{K}_{\mathcal{T}\mathcal{F}} \\ \mathcal{K}_{\mathcal{F}\mathcal{T}} & \mathcal{K}_{\mathcal{F}} \end{bmatrix} \begin{bmatrix} \mathbf{U}_{\mathcal{T}}^{n,j} \\ \mathbf{U}_{\mathcal{F}}^{n,j} \end{bmatrix} \right)$$

► Each stage can be rewritten as

$$\begin{bmatrix} \mathcal{M}_{\mathcal{T}} + a_* \Delta t \mathcal{K}_{\mathcal{T}} & a_* \Delta t \mathcal{K}_{\mathcal{T}\mathcal{F}} \\ a_* \Delta t \mathcal{K}_{\mathcal{F}\mathcal{T}} & a_* \Delta t \mathcal{K}_{\mathcal{F}} \end{bmatrix} \begin{bmatrix} \mathbf{U}_{\mathcal{T}}^{n,i} \\ \mathbf{U}_{\mathcal{F}}^{n,i} \end{bmatrix} = \begin{bmatrix} \mathbf{B}_{\mathcal{T}}^{n,i} \\ \mathbf{B}_{\mathcal{F}}^{n,i} \end{bmatrix}$$

■ **SDIRK($s, s + 1$) schemes:** For all $i \in \{1, \dots, s\}$,

$$\begin{bmatrix} \mathcal{M}_{\mathcal{T}} & 0 \\ 0 & 0 \end{bmatrix} \begin{bmatrix} \mathbf{U}_{\mathcal{T}}^{n,i} \\ \mathbf{U}_{\mathcal{F}}^{n,i} \end{bmatrix} = \begin{bmatrix} \mathcal{M}_{\mathcal{T}} & 0 \\ 0 & 0 \end{bmatrix} \begin{bmatrix} \mathbf{U}_{\mathcal{T}}^{n-1} \\ \mathbf{U}_{\mathcal{F}}^{n-1} \end{bmatrix} + \Delta t \sum_{j=1}^{\textcolor{red}{i}} a_{ij} \left(\begin{bmatrix} \mathbf{F}_{\mathcal{T}}^{n-1+c_j} \\ 0 \end{bmatrix} - \begin{bmatrix} \mathcal{K}_{\mathcal{T}} & \mathcal{K}_{\mathcal{T}\mathcal{F}} \\ \mathcal{K}_{\mathcal{F}\mathcal{T}} & \mathcal{K}_{\mathcal{F}} \end{bmatrix} \begin{bmatrix} \mathbf{U}_{\mathcal{T}}^{n,j} \\ \mathbf{U}_{\mathcal{F}}^{n,j} \end{bmatrix} \right)$$

► Each stage can be rewritten as

$$\begin{bmatrix} \mathcal{M}_{\mathcal{T}} + a_* \Delta t \mathcal{K}_{\mathcal{T}} & a_* \Delta t \mathcal{K}_{\mathcal{T}\mathcal{F}} \\ a_* \Delta t \mathcal{K}_{\mathcal{F}\mathcal{T}} & a_* \Delta t \mathcal{K}_{\mathcal{F}} \end{bmatrix} \begin{bmatrix} \mathbf{U}_{\mathcal{T}}^{n,i} \\ \mathbf{U}_{\mathcal{F}}^{n,i} \end{bmatrix} = \begin{bmatrix} \mathbf{B}_{\mathcal{T}}^{n,i} \\ \mathbf{B}_{\mathcal{F}}^{n,i} \end{bmatrix}$$

■ **Usual static condensation: Cell dofs elimination**

- Global system coupling only face dofs
- Cheap local postprocessing to recover cell dofs

■ **ERK(s) schemes:** For all $i \in \{1, \dots, s\}$,

$$\begin{bmatrix} \mathcal{M}_{\mathcal{T}} & 0 \\ 0 & 0 \end{bmatrix} \begin{bmatrix} \mathbf{U}_{\mathcal{T}}^{n,i} \\ \mathbf{U}_{\mathcal{F}}^{n,i} \end{bmatrix} = \begin{bmatrix} \mathcal{M}_{\mathcal{T}} & 0 \\ 0 & 0 \end{bmatrix} \begin{bmatrix} \mathbf{U}_{\mathcal{T}}^{n-1} \\ \mathbf{U}_{\mathcal{F}}^{n-1} \end{bmatrix} + \Delta t \sum_{j=1}^{\textcolor{red}{i-1}} a_{ij} \left(\begin{bmatrix} \mathbf{F}_{\mathcal{T}}^{n-1+c_j} \\ 0 \end{bmatrix} - \begin{bmatrix} \mathcal{K}_{\mathcal{T}} & \mathcal{K}_{\mathcal{T}\mathcal{F}} \\ \mathcal{K}_{\mathcal{F}\mathcal{T}} & \mathcal{K}_{\mathcal{F}} \end{bmatrix} \begin{bmatrix} \mathbf{U}_{\mathcal{T}}^{n,j} \\ \mathbf{U}_{\mathcal{F}}^{n,j} \end{bmatrix} \right)$$

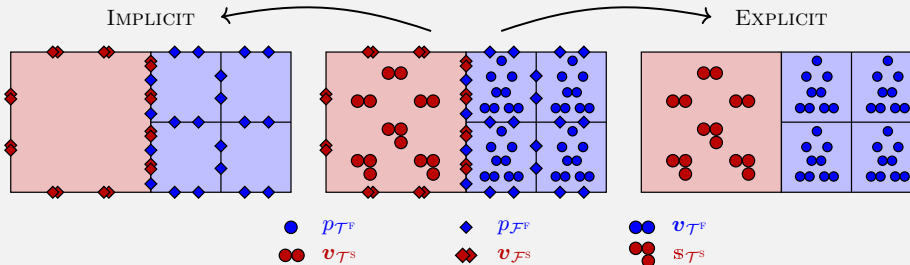
► **Face dofs elimination:** $\mathcal{K}_{\mathcal{F}} \mathbf{U}_{\mathcal{F}}^{n,j} = -\mathcal{K}_{\mathcal{F}\mathcal{T}} \mathbf{U}_{\mathcal{T}}^{n,j}$

■ **ERK(s) schemes:** For all $i \in \{1, \dots, s\}$,

$$\begin{bmatrix} \mathcal{M}_T & 0 \\ 0 & 0 \end{bmatrix} \begin{bmatrix} U_T^{n,i} \\ U_{\mathcal{F}}^{n,i} \end{bmatrix} = \begin{bmatrix} \mathcal{M}_T & 0 \\ 0 & 0 \end{bmatrix} \begin{bmatrix} U_T^{n-1} \\ U_{\mathcal{F}}^{n-1} \end{bmatrix} + \Delta t \sum_{j=1}^{\textcolor{red}{i-1}} a_{ij} \left(\begin{bmatrix} F_T^{n-1+c_j} \\ 0 \end{bmatrix} - \begin{bmatrix} \mathcal{K}_T & \mathcal{K}_{T\mathcal{F}} \\ \mathcal{K}_{\mathcal{F}T} & \mathcal{K}_{\mathcal{F}} \end{bmatrix} \begin{bmatrix} U_T^{n,j} \\ U_{\mathcal{F}}^{n,j} \end{bmatrix} \right)$$

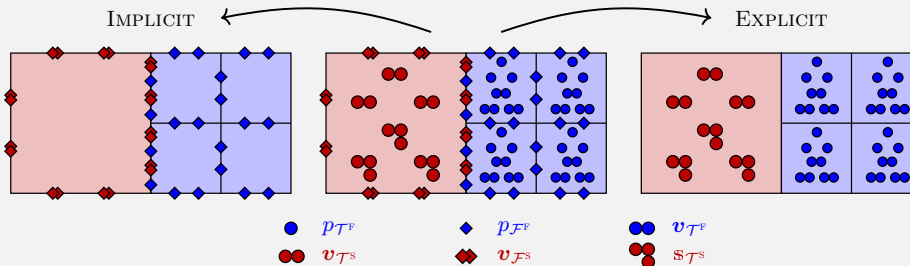
- ▶ **Face dofs elimination:** $\mathcal{K}_{\mathcal{F}} U_{\mathcal{F}}^{n,j} = -\mathcal{K}_{\mathcal{F}T} U_T^{n,j}$
- ▶ Each stage becomes (**dG rewriting by static condensation**):

$$\mathcal{M}_T U_T^{n,i} = \mathcal{M}_T U_T^{n-1} + \Delta t \sum_{j=1}^{\textcolor{red}{i-1}} a_{ij} \left(F_T^{n-1+c_j} - (\mathcal{K}_T - \mathcal{K}_{T\mathcal{F}} \mathcal{K}_{\mathcal{F}}^{-1} \mathcal{K}_{\mathcal{F}T}) U_T^{n,j} \right)$$



■ Proportion
of face dofs:

		MIXED-ORDER			EQUAL-ORDER			$k \gg 1$
		$k = 1$	$k = 2$	$k = 3$	$k = 1$	$k = 2$	$k = 3$	
2D	ACOUSTIC	20%	17%	15%	25%	20%	17%	$\frac{1}{k}$
	ELASTIC	22%	19%	17%	29%	23%	19%	$\frac{6}{5k}$
3D	ACOUSTIC	21%	19%	17%	27%	23%	20%	$\frac{3}{2k}$
	ELASTIC	25%	23%	21%	33%	29%	25%	$\frac{2}{k}$



■ Proportion
of face dofs:

		MIXED-ORDER			EQUAL-ORDER			$k \gg 1$
		$k = 1$	$k = 2$	$k = 3$	$k = 1$	$k = 2$	$k = 3$	
2D	ACOUSTIC	20%	17%	15%	25%	20%	17%	$\frac{1}{k}$
	ELASTIC	22%	19%	17%	29%	23%	19%	$\frac{6}{5k}$
3D	ACOUSTIC	21%	19%	17%	27%	23%	20%	$\frac{3}{2k}$
	ELASTIC	25%	23%	21%	33%	29%	25%	$\frac{2}{k}$

→ Elimination of cell dofs much more efficient than face dofs

II.4. Discretization choices

■ Implicit discretization

- ▶ Mixed-order discretization:
 - More unknowns but eliminated by static condensation
 - More efficient than equal-order with specific HHO stabilization
- for elliptic problems see  [Cicuttin, Ern, Pignet \(2021\)](#)

II.4. Discretization choices

■ Implicit discretization

- ▶ Mixed-order discretization:
 - More unknowns but eliminated by static condensation
 - More efficient than equal-order with specific HHO stabilization
for elliptic problems see  [Cicuttin, Ern, Pignet \(2021\)](#)
- ▶ Lehrenfeld–Schöberl $\mathcal{O}(\frac{1}{h})$ -stabilization
 - Dual unknowns converge at $\mathcal{O}(h^{k+1})$ in L^2 -norm
 - Primal unknowns converge at $\mathcal{O}(h^{k+2})$ in L^2 -norm (**superconvergence numerically observed**)

II.4. Discretization choices

■ Implicit discretization

- ▶ Mixed-order discretization:
 - More unknowns but eliminated by static condensation
 - More efficient than equal-order with specific HHO stabilization
for elliptic problems see  [Cicuttin, Ern, Pignet \(2021\)](#)
- ▶ Lehrenfeld–Schöberl $\mathcal{O}(\frac{1}{h})$ -stabilization
 - Dual unknowns converge at $\mathcal{O}(h^{k+1})$ in L^2 -norm
 - Primal unknowns converge at $\mathcal{O}(h^{k+2})$ in L^2 -norm (**superconvergence numerically observed**)

■ Explicit discretization

- ▶ Equal-order discretization: → Less degrees of freedom

II.4. Discretization choices

■ Implicit discretization

- ▶ Mixed-order discretization:
 - More unknowns but eliminated by static condensation
 - More efficient than equal-order with specific HHO stabilization
for elliptic problems see  [Cicuttin, Ern, Pignet \(2021\)](#)
- ▶ Lehrenfeld–Schöberl $\mathcal{O}(\frac{1}{h})$ -stabilization
 - Dual unknowns converge at $\mathcal{O}(h^{k+1})$ in L^2 -norm
 - Primal unknowns converge at $\mathcal{O}(h^{k+2})$ in L^2 -norm (**superconvergence numerically observed**)

■ Explicit discretization

- ▶ Equal-order discretization: → Less degrees of freedom
- ▶ Plain Least-Squares stabilization: → Ensure block-diagonal structure

II.4. Discretization choices

■ Implicit discretization

- ▶ Mixed-order discretization:
 - More unknowns but eliminated by static condensation
 - More efficient than equal-order with specific HHO stabilization
for elliptic problems see  [Cicuttin, Ern, Pignet \(2021\)](#)
- ▶ Lehrenfeld–Schöberl $\mathcal{O}(\frac{1}{h})$ -stabilization
 - Dual unknowns converge at $\mathcal{O}(h^{k+1})$ in L^2 -norm
 - Primal unknowns converge at $\mathcal{O}(h^{k+2})$ in L^2 -norm (**superconvergence numerically observed**)

■ Explicit discretization

- ▶ Equal-order discretization: → Less degrees of freedom
- ▶ Plain Least-Squares stabilization: → Ensure block-diagonal structure
- ▶ $\mathcal{O}(1)$ -stabilization: → Reasonable CFL condition: $\Delta t = \mathcal{O}(h)$

II.5. Numerical results

■ Academic tests cases

- ▶ CFL stability limit
- ▶ Convergences rates

■ Ricker wavelet in bilayered domain

- ▶ Validation by comparison to semi-analytical solution (**Gar6more**)
- ▶ Efficiency: Implicit vs. Explicit

■ Ricker wavelet in sedimentary basin

- ▶ Illustration of HHO mesh flexibility
- ▶ Comparison to a reference solver (**SEM2D**)

II.5. Numerical results

■ Academic tests cases

- ▶ CFL stability limit
- ▶ Convergences rates

■ Ricker wavelet in bilayered domain

- ▶ Validation by comparison to semi-analytical solution (**Gar6more**)
- ▶ Efficiency: Implicit vs. Explicit

■ Ricker wavelet in sedimentary basin

- ▶ Illustration of HHO mesh flexibility
- ▶ Comparison to a reference solver (**SEM2D**)

■ Creation of a new branch in disk++ library (<https://github.com/wareHH0use/diskpp>)

- ▶ Data structures, Discrete operators, Assembly processes,
Interfacing with various solvers and Preconditioners, and Post-processing

II.5. Numerical results

■ Academic tests cases

- ▶ CFL stability limit
- ▶ Convergences rates

■ Ricker wavelet in bilayered domain

- ▶ Validation by comparison to semi-analytical solution (**Gar6more**)
- ▶ Efficiency: Implicit vs. Explicit

■ Ricker wavelet in sedimentary basin

- ▶ Illustration of HHO mesh flexibility
- ▶ Comparison to a reference solver (**SEM2D**)

■ Creation of a new branch in disk++ library (<https://github.com/wareHHOuse/diskpp>)

- ▶ Data structures, Discrete operators, Assembly processes,
Interfacing with various solvers and Preconditioners, and Post-processing

■ Not discussed:

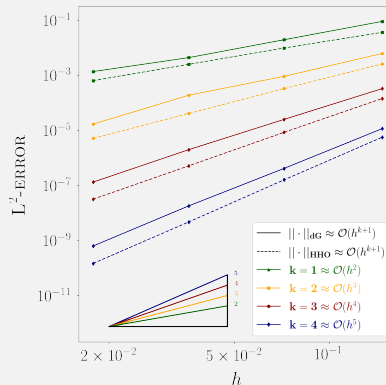
- ▶ Spectral analysis & Study of the energy dissipation
- ▶ Implementation of a 3D spectral HDG method for elastodynamics in HPC code

Academic test case

■ Convergence rates on general meshes: recover theoretical rates

Explicit schemes with $\mathcal{O}(1)$ -stabilization:

$$\|\cdot\|_{dG}: \mathcal{O}(h^{k+1}) \quad \|\cdot\|_{HHO}: \mathcal{O}(h^{k+1})$$



Academic test case

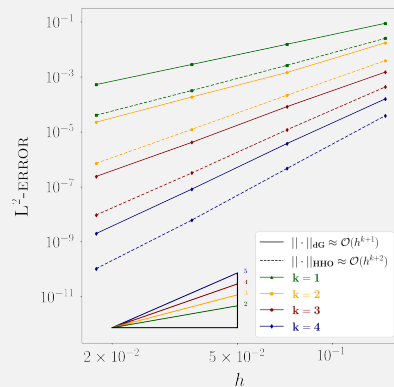
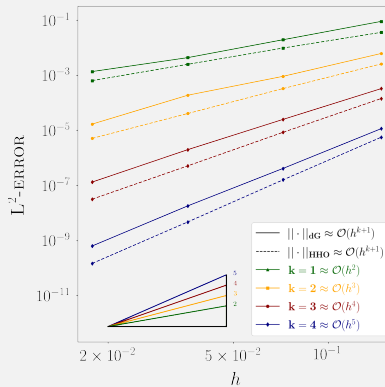
■ Convergence rates on general meshes: recover theoretical rates

Explicit schemes with $\mathcal{O}(1)$ -stabilization:

$$\|\cdot\|_{\text{dG}}: \mathcal{O}(h^{k+1}) \quad \|\cdot\|_{\text{HHO}}: \mathcal{O}(h^{k+1})$$

Implicit schemes with $\mathcal{O}(\frac{1}{h})$ -stabilization:

$$\|\cdot\|_{\text{dG}}: \mathcal{O}(h^{k+1}) \quad \|\cdot\|_{\text{HHO}}: \mathcal{O}(h^{k+2})$$

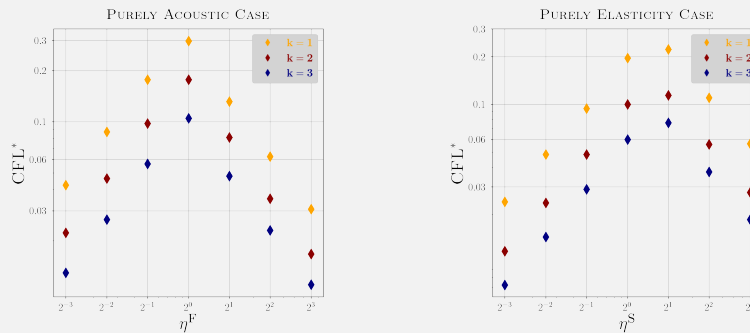


- Impact of stabilization on CFL stability limit: $c_{\sharp} \frac{\Delta t}{h} \leq \text{CFL}^*(s, k, \eta^f, \eta^s)$

■ Impact of stabilization on CFL stability limit: $c_{\sharp} \frac{\Delta t}{h} \leq \text{CFL}^*(s, k, \eta^F, \eta^S)$

► Weighted $\mathcal{O}(1)$ -stabilization with $\eta^{F/S} := 2^m$ with $m \in [-3, 3]$

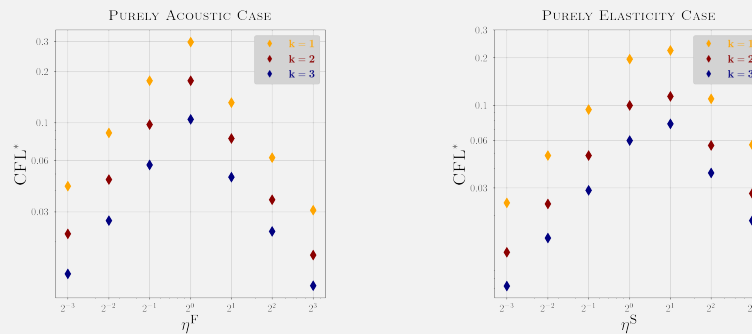
$$\tilde{s}_{\mathcal{M}^F}(\hat{p}_{\mathcal{M}^F}, \hat{q}_{\mathcal{M}^F}) := \eta^F s_{\mathcal{M}^F}(\hat{p}_{\mathcal{M}^F}, \hat{q}_{\mathcal{M}^F}), \quad \tilde{s}_{\mathcal{M}^S}(\hat{v}_{\mathcal{M}^S}, \hat{w}_{\mathcal{M}^S}) := \eta^S s_{\mathcal{M}^S}(\hat{v}_{\mathcal{M}^S}, \hat{w}_{\mathcal{M}^S})$$



■ Impact of stabilization on CFL stability limit: $c_{\sharp} \frac{\Delta t}{h} \leq \text{CFL}^*(s, k, \eta^f, \eta^s)$

► Weighted $\mathcal{O}(1)$ -stabilization with $\eta^{F/S} := 2^m$ with $m \in [-3, 3]$

$$\tilde{s}_{\mathcal{M}^F}(\hat{p}_{\mathcal{M}^F}, \hat{q}_{\mathcal{M}^F}) := \eta^F s_{\mathcal{M}^F}(\hat{p}_{\mathcal{M}^F}, \hat{q}_{\mathcal{M}^F}), \quad \tilde{s}_{\mathcal{M}^S}(\hat{v}_{\mathcal{M}^S}, \hat{w}_{\mathcal{M}^S}) := \eta^S s_{\mathcal{M}^S}(\hat{v}_{\mathcal{M}^S}, \hat{w}_{\mathcal{M}^S})$$



- Evolution of CFL^* as $\min(\eta, 1/\eta)$ → Optimal CFL for $\eta^F \approx 1 \approx \eta^S$
- $\eta^{f/s} \gg 1 \sim \mathcal{O}(\frac{1}{h})$ -stabilization → degrades CFL

Influence of cell geometry

MESHES	$s = 2$			$s = 3$			$s = 4$			
	\triangle	\square	\diamond	\triangle	\square	\diamond	\triangle	\square	\diamond	
$k = 1$	CFL*	0.191	0.205	0.264	0.238	0.253	0.329	0.265	0.282	0.363
	RATIO	1	1.07	1.38	1	1.06	1.38	1	1.06	1.37
$k = 2$	CFL*	0.106	0.099	0.136	0.133	0.123	0.170	0.147	0.138	0.188
	RATIO	1	0.93	1.28	1	0.92	1.28	1	0.94	1.28
$k = 3$	CFL*	0.072	0.063	0.082	0.090	0.079	0.102	0.100	0.087	0.115
	RATIO	1	0.88	1.13	1	0.88	1.13	1	0.87	1.15

■ Influence of cell geometry

MESHES	$s = 2$			$s = 3$			$s = 4$			
	\triangle	\square	\diamond	\triangle	\square	\diamond	\triangle	\square	\diamond	
$k = 1$	CFL*	0.191	0.205	0.264	0.238	0.253	0.329	0.265	0.282	0.363
	RATIO	1	1.07	1.38	1	1.06	1.38	1	1.06	1.37
$k = 2$	CFL*	0.106	0.099	0.136	0.133	0.123	0.170	0.147	0.138	0.188
	RATIO	1	0.93	1.28	1	0.92	1.28	1	0.94	1.28
$k = 3$	CFL*	0.072	0.063	0.082	0.090	0.079	0.102	0.100	0.087	0.115
	RATIO	1	0.88	1.13	1	0.88	1.13	1	0.87	1.15

- ▶ CFL* mildly sensitive to mesh geometry
- ▶ CFL improvement for meshes with higher face counts if $k = 1$
- ▶ Less pronounced improvement for $k \geq 2$

Propagation of a Ricker wavelet in a bilayered domain

■ Test case setting

- ▶ $\mathbf{v}_0(x, y) := \theta \exp\left(-\pi^2 \frac{r^2}{\lambda^2}\right) (x - x_c, y - y_c)^\dagger$
- ▶ Fluid subdomain: **Water**
- ▶ Solid subdomain: **Hardrock (Granite)**



Propagation of a Ricker wavelet in a bilayered domain

■ Test case setting

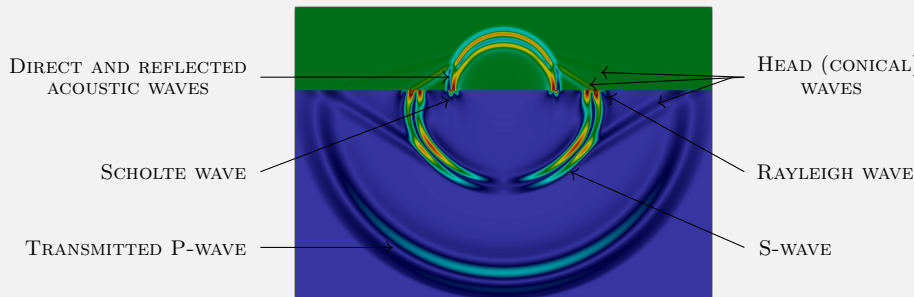
- ▶ $\mathbf{v}_0(x, y) := \theta \exp\left(-\pi^2 \frac{r^2}{\lambda^2}\right) (x - x_c, y - y_c)^\dagger$
- ▶ Fluid subdomain: **Water**
- ▶ Solid subdomain: **Hardrock (Granite)**



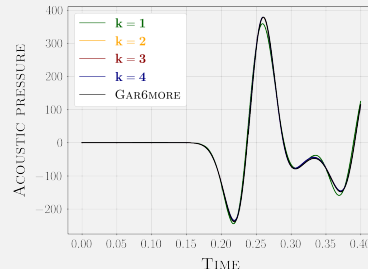
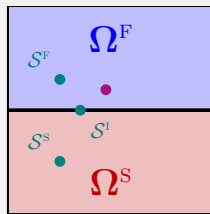
Propagation of a Ricker wavelet in a bilayered domain

■ Test case setting

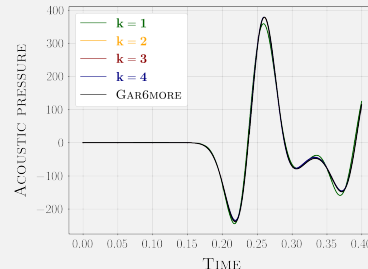
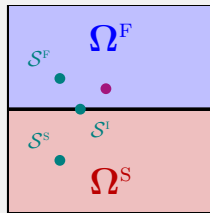
- ▶ $\mathbf{v}_0(x, y) := \theta \exp\left(-\pi^2 \frac{r^2}{\lambda^2}\right)(x - x_c, y - y_c)^\dagger$
- ▶ Fluid subdomain: **Water**
- ▶ Solid subdomain: **Hardrock (Granite)**



■ Comparison to semi-analytical solution (Gar6more) Diaz, Ezziani (2008)



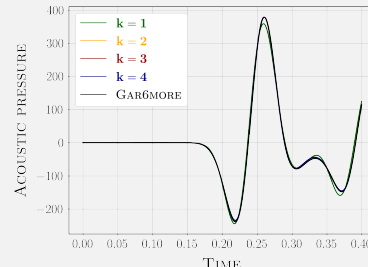
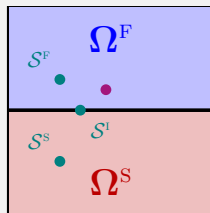
■ Comparison to semi-analytical solution (Gar6more) Diaz, Ezziani (2008)



■ Efficiency study: Fair comparison (for 3D perspective)

- ▶ Implicit schemes with **iterative (BiCG) solver** (with ILU preconditioner)
- ▶ Explicit schemes with **time step just below stability limit**

■ Comparison to semi-analytical solution (Gar6more) Diaz, Ezziani (2008)



■ Efficiency study: Fair comparison (for 3D perspective)

- ▶ Implicit schemes with **iterative (BiCG) solver** (with ILU preconditioner)
- ▶ Explicit schemes with **time step just below stability limit**

▶ Implicit time steps:
almost 7× larger

▶ Implicit schemes:
decrease by 25%
CPU time

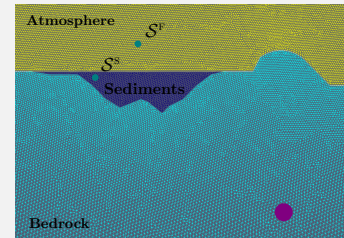
▶ **To be confirmed in 3D**

SCHEMES	SOLVER	CFL*	$\frac{\Delta t}{c_s h}$	RATIO	CPU [s]	RATIO	ERR	
SDIRK(3,4)	$k = 2$ $k = 3$	direct	n/a	0.414	6.90	1125	1	3.15e-02
				0.414	6.90	2284	2.03	2.52e-02
SDIRK(3,4)	$k = 2$ $k = 3$	iterative	n/a	0.414	6.90	2228	1.98	3.91e-02
				0.414	6.90	4216	3.75	3.11e-02
ERK(4)	$k = 2$ $k = 3$	n/a	0.138	0.095	1.36	1533	1.27	2.01e-2
			0.087	0.060	1	5664	5.03	1.90e-2

Propagation of a Ricker wavelet in a sedimentary basin

■ Test case setting

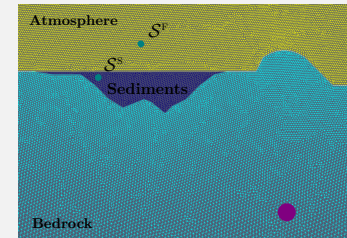
MATERIAL	$\rho^{\text{F/S}} \left[\frac{\text{kg}}{\text{m}^3} \right]$	$c_p^{\text{F/S}} \left[\frac{\text{m}}{\text{s}} \right]$	$c_p^{\text{S}} \left[\frac{\text{m}}{\text{s}} \right]$
ATMOSPHERE	1.225	343	n/a
SEDIMENTS	1300	1600	900
BEDROCK	2570	5350	3009



Propagation of a Ricker wavelet in a sedimentary basin

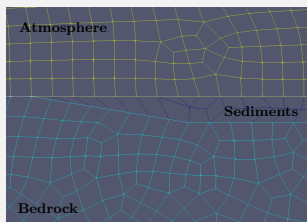
■ Test case setting

MATERIAL	$\rho^F/S \left[\frac{\text{kg}}{\text{m}^3} \right]$	$c_p^F/S \left[\frac{\text{m}}{\text{s}} \right]$	$c_p^S \left[\frac{\text{m}}{\text{s}} \right]$
ATMOSPHERE	1.225	343	n/a
SEDIMENTS	1300	1600	900
BEDROCK	2570	5350	3009

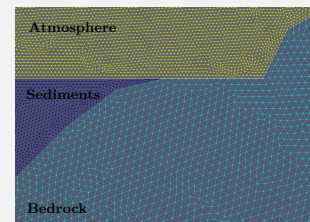


→ Illustration of HHO mesh flexibility: Typical geometry difficult to mesh in 3D

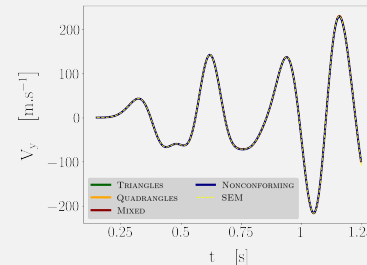
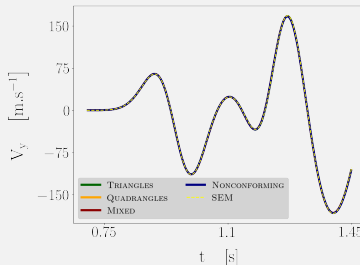
■ Mixed meshes



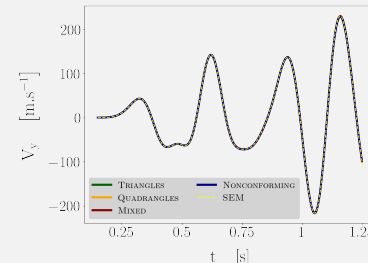
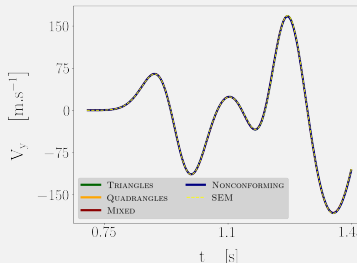
■ Nonconforming meshes with hanging nodes



■ Comparison with a reference spectral solver



■ Comparison with a reference spectral solver



■ Wave trapped into sedimentary basin

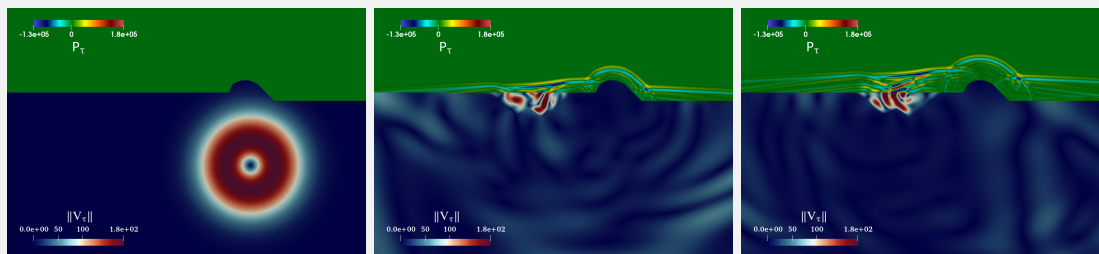


Table of Contents

III - Unfitted HHO stabilized by polynomial extension

II.1 Motivation & model problem

II.2 Unfitted FEM

II.3 Unfitted HHO

II.4 Polynomial extension

II.5 Numerical results



E. Burman, A. Ern, R. Mottier (2025). Submitted to SINUM

*Unfitted hybrid high-order methods stabilized by polynomial
extension for elliptic interface problems*

III.1. Motivation & model problem

- **Goal:** Accurate simulation of elasto-acoustic waves in **heterogeneous domains with complex geometries**

III.1. Motivation & model problem

- **Goal:** Accurate simulation of elasto-acoustic waves in **heterogeneous domains with complex geometries**
- **HHO methods:**
 - ✓ Allow for efficient implicit and explicit time discretizations
 - ✓ Work on general meshes
 - ✗ Polytopal methods work optimally on planar faces

III.1. Motivation & model problem

- **Goal:** Accurate simulation of elasto-acoustic waves in **heterogeneous domains with complex geometries**
- **HHO methods:** ✓ Allow for efficient implicit and explicit time discretizations
✓ Work on general meshes
✗ Polytopal methods work optimally on planar faces

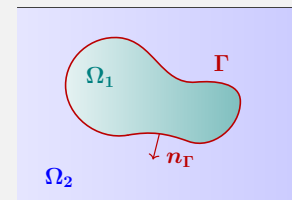
▲ What if interfaces cannot be meshed with planar faces

Idea: Use of unfitted HHO methods to handle curved interfaces

■ First step towards wave equation: **Elliptic interface problem**

► Strong form:

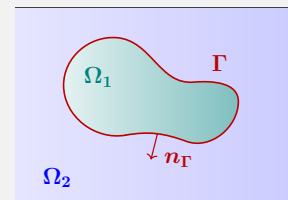
$$\begin{cases} -\nabla \cdot (\kappa \nabla p) = f & \text{in } \Omega_1 \cup \Omega_2 \\ [\![p]\!]_{\Gamma} = g_D & \text{on } \Gamma \\ [\![\kappa \nabla p]\!]_{\Gamma} \cdot \mathbf{n}_{\Gamma} = g_N & \text{on } \Gamma \\ p = 0 & \text{on } \partial\Omega \end{cases}$$



■ First step towards wave equation: Elliptic interface problem

► Strong form:

$$\begin{cases} -\nabla \cdot (\kappa \nabla p) = f & \text{in } \Omega_1 \cup \Omega_2 \\ \llbracket p \rrbracket_{\Gamma} = g_D & \text{on } \Gamma \\ \llbracket \kappa \nabla p \rrbracket_{\Gamma} \cdot \mathbf{n}_{\Gamma} = g_N & \text{on } \Gamma \\ p = 0 & \text{on } \partial\Omega \end{cases}$$

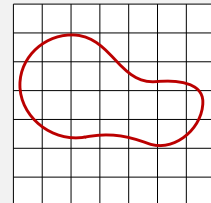


► Weak form: Find $p \in H^1(\Omega_1 \cup \Omega_2)$, such that $\llbracket p \rrbracket_{\Gamma} = g_D$ and $\mathbf{a}(p, q) = \ell(q)$ with

- $\mathbf{a}(p, q) := \sum_{i \in \{1, 2\}} (\kappa \nabla p_i, \nabla q_i)_{\Omega_i}$
- $\ell(q) := (f, q)_{\Omega} + (g_N, q)_{\Gamma}$

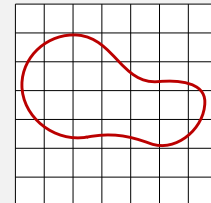
III.2. Unfitted FEM: Basic concepts

- Main idea: Minimize complexity of mesh generation
 - ▶ Mesh cells arbitrarily cut by physical interfaces



III.2. Unfitted FEM: Basic concepts

- Main idea: Minimize complexity of mesh generation
 - ▶ Mesh cells arbitrarily cut by physical interfaces



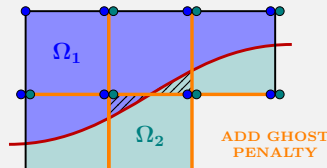
■ Unfitted FEM

- ▶ Handle cut cells by doubling unknowns: (maintain optimality)

[Hansbo, Hansbo \(2002\)](#)

- ▶ Ill-cut cell stabilization: Ghost penalty

[Burman \(2010\)](#)



III.3. Unfitted HHO

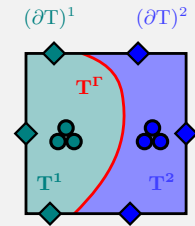
- **Seminal papers:**  [Burman, Ern \(2018\)](#)  [Burman, Cicuttin, Delay, Ern \(2021\)](#)
- **Different applications:** Stokes interface problems  [Burman, Delay, Ern \(2021\)](#)
Wave propagation (second-order form)  [Burman, Duran, Ern \(2022b\)](#)

III.3. Unfitted HHO

- Seminal papers: Burman, Ern (2018) Burman, Cicuttin, Delay, Ern (2021)
- Different applications: Stokes interface problems Burman, Delay, Ern (2021)
Wave propagation (second-order form) Burman, Duran, Ern (2022b)

Doubling cell and face unknowns in cut cells:

$$\hat{p}_T := (\hat{p}_{T^1}, \hat{p}_{T^2}) := (p_{T^1}, p_{(\partial T)^1}, p_{T^2}, p_{(\partial T)^2}) \in \hat{P}_T^k := \hat{P}_{T^1}^k \times \hat{P}_{T^2}^k$$

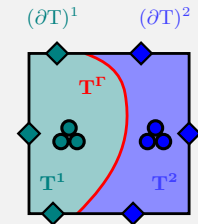


III.3. Unfitted HHO

- Seminal papers: Burman, Ern (2018) Burman, Cicuttin, Delay, Ern (2021)
- Different applications: Stokes interface problems Burman, Delay, Ern (2021)
Wave propagation (second-order form) Burman, Duran, Ern (2022b)

■ Doubling cell and face unknowns in cut cells:

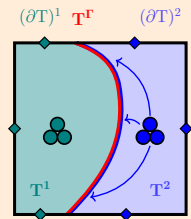
$$\hat{p}_T := (\hat{p}_{T^1}, \hat{p}_{T^2}) := (p_{T^1}, p_{(\partial T)^1}, p_{T^2}, p_{(\partial T)^2}) \in \hat{P}_T^k := \hat{P}_{T^1}^k \times \hat{P}_{T^2}^k$$



■ No unknown attached to interface

- ▶ Need of mixed-order discretization: $k' = k + 1$

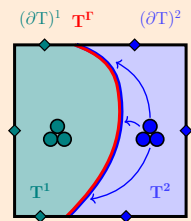
■ Notation: $T^i := T \cap \Omega^i$, $(\partial T)^i := \partial T \cap \Omega^i$, $T^\Gamma := \partial T \cap \Gamma$



■ Notation: $T^i := T \cap \Omega^i$, $(\partial T)^i := \partial T \cap \Omega^i$, $T^\Gamma := \partial T \cap \Gamma$

■ Gradient reconstruction

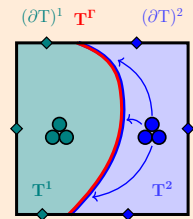
- Gradient is reconstructed in each sub-cell



■ Notation: $T^i := T \cap \Omega^i$, $(\partial T)^i := \partial T \cap \Omega^i$, $T^\Gamma := \partial T \cap \Gamma$

■ Gradient reconstruction

- ▶ Gradient is reconstructed in each sub-cell
- ▶ Jump across interface is accounted for in gradient reconstruction and close integration by parts

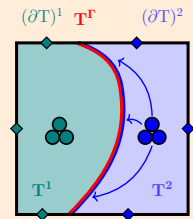


$$(\mathbf{g}_{T^i}(\hat{p}_T), \mathbf{q})_{T^i} := (\nabla p_{T^i}, \mathbf{q})_{T^i} + (p_{(\partial T)^i} - p_{T^i}, \mathbf{q} \cdot \mathbf{n}_T)_{(\partial T)^i} - \delta_{i1}([\![p_T]\!]_\Gamma, \mathbf{q} \cdot \mathbf{n}_\Gamma)_{T^\Gamma}$$

■ Notation: $T^i := T \cap \Omega^i$, $(\partial T)^i := \partial T \cap \Omega^i$, $T^\Gamma := \partial T \cap \Gamma$

■ Gradient reconstruction

- ▶ Gradient is reconstructed in each sub-cell
- ▶ Jump across interface is accounted for in gradient reconstruction and close integration by parts



$$(g_{T^i}(\hat{p}_T), \mathbf{q})_{T^i} := (\nabla p_{T^i}, \mathbf{q})_{T^i} + (p_{(\partial T)^i} - p_{T^i}, \mathbf{q} \cdot \mathbf{n}_T)_{(\partial T)^i} - \delta_{i1}([\![p_T]\!]_\Gamma, \mathbf{q} \cdot \mathbf{n}_\Gamma)_{T^\Gamma}$$

- ▶ Robustness wrt contrast $\kappa_1 \ll \kappa_2$: non-symmetric inclusion of $[\![p_T]\!]_\Gamma$

■ Stabilization

- Usual mixed-order LS $\mathcal{O}(\frac{1}{h})$ -stabilization (on internal faces):

$$s_{\mathcal{M}}^{\circ}(\hat{p}_{\mathcal{M}}, \hat{q}_{\mathcal{M}}) := \sum_{T \in \mathcal{T}} \sum_{i \in \{1,2\}} \frac{\kappa_i}{h_T} (\Pi_{(\partial T)^i}^k (p_{T^i} - p_{(\partial T)^i}), q_{T^i} - q_{(\partial T)^i})_{(\partial T)^i}$$

■ Stabilization

- ▶ Usual mixed-order LS $\mathcal{O}(\frac{1}{h})$ -stabilization (on internal faces):

$$s_{\mathcal{M}}^{\circ}(\hat{p}_{\mathcal{M}}, \hat{q}_{\mathcal{M}}) := \sum_{T \in \mathcal{T}} \sum_{i \in \{1,2\}} \frac{\kappa_i}{h_T} (\Pi_{(\partial T)^i}^k (p_{T^i} - p_{(\partial T)^i}), q_{T^i} - q_{(\partial T)^i})_{(\partial T)^i}$$

- ▶ Nitsche-like penalty (at interfaces):

$$s_{\mathcal{M}}^{\Gamma}(\hat{p}_{\mathcal{M}}, \hat{q}_{\mathcal{M}}) := \sum_{T \in \mathcal{T}} \delta_{i1} \frac{\kappa_1}{h_T} ([\![p_T]\!], [\![q_T]\!])_{T^\Gamma}$$

■ Stabilization

- Usual mixed-order LS $\mathcal{O}(\frac{1}{h})$ -stabilization (on internal faces):

$$s_{\mathcal{M}}^{\circ}(\hat{p}_{\mathcal{M}}, \hat{q}_{\mathcal{M}}) := \sum_{T \in \mathcal{T}} \sum_{i \in \{1,2\}} \frac{\kappa_i}{h_T} (\Pi_{(\partial T)^i}^k (p_{T^i} - p_{(\partial T)^i}), q_{T^i} - q_{(\partial T)^i})_{(\partial T)^i}$$

- Nitsche-like penalty (at interfaces):

$$s_{\mathcal{M}}^{\Gamma}(\hat{p}_{\mathcal{M}}, \hat{q}_{\mathcal{M}}) := \sum_{T \in \mathcal{T}} \delta_{i1} \frac{\kappa_1}{h_T} ([\![p_T]\!], [\![q_T]\!])_{T^\Gamma}$$

- Total stabilization:

$$s_{\mathcal{M}}(\hat{p}_{\mathcal{M}}, \hat{q}_{\mathcal{M}}) := s_{\mathcal{M}}^{\circ}(\hat{p}_{\mathcal{M}}, \hat{q}_{\mathcal{M}}) + s_{\mathcal{M}}^{\Gamma}(\hat{p}_{\mathcal{M}}, \hat{q}_{\mathcal{M}})$$

■ Discrete problem: $a_{\mathcal{M}}(\hat{p}_{\mathcal{M}}, \hat{q}_{\mathcal{M}}) := \ell_{\mathcal{M}}(\hat{q}_{\mathcal{M}})$

► Discrete bilinear form:

$$a_{\mathcal{M}}(\hat{p}_{\mathcal{M}}, \hat{q}_{\mathcal{M}}) := \sum_{T \in \mathcal{T}} \sum_{i \in \{1, 2\}} \kappa_i(\mathbf{g}_{T^i}(\hat{p}_{\mathcal{M}}), \mathbf{g}_{T^i}(\hat{q}_{\mathcal{M}}))_{T^i} + s_{\mathcal{M}}(\hat{p}_{\mathcal{M}}, \hat{q}_{\mathcal{M}})$$

■ Discrete problem: $a_{\mathcal{M}}(\hat{p}_{\mathcal{M}}, \hat{q}_{\mathcal{M}}) := \ell_{\mathcal{M}}(\hat{q}_{\mathcal{M}})$

► Discrete bilinear form:

$$a_{\mathcal{M}}(\hat{p}_{\mathcal{M}}, \hat{q}_{\mathcal{M}}) := \sum_{T \in \mathcal{T}} \sum_{i \in \{1,2\}} \kappa_i(\mathbf{g}_{T^i}(\hat{p}_{\mathcal{M}}), \mathbf{g}_{T^i}(\hat{q}_{\mathcal{M}}))_{T^i} + s_{\mathcal{M}}(\hat{p}_{\mathcal{M}}, \hat{q}_{\mathcal{M}})$$

► Discrete linear form (with $\ell_{\mathcal{M}}$ defined so as to ensure consistency):

$$\ell_{\mathcal{M}}(\hat{q}_{\mathcal{M}}) := \sum_{T \in \mathcal{T}} \sum_{i \in \{1,2\}} (f, w_{T^i})_{T^i} + \sum_{T \in \mathcal{T}^{\text{cut}}} (g_N, q_{T^2})_{T^{\Gamma}} + \sum_{T \in \mathcal{T}^{\text{cut}}} \kappa_1(g_D, [\![q_T]\!] h_T^{-1} - \mathbf{g}_{T^1} \cdot \mathbf{n}_{\Gamma})_{T^{\Gamma}}$$

■ Discrete problem: $a_{\mathcal{M}}(\hat{p}_{\mathcal{M}}, \hat{q}_{\mathcal{M}}) := \ell_{\mathcal{M}}(\hat{q}_{\mathcal{M}})$

► Discrete bilinear form:

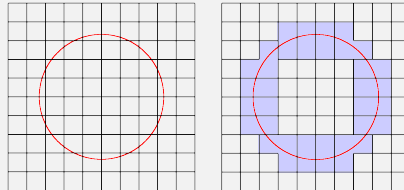
$$a_{\mathcal{M}}(\hat{p}_{\mathcal{M}}, \hat{q}_{\mathcal{M}}) := \sum_{T \in \mathcal{T}} \sum_{i \in \{1,2\}} \kappa_i(\mathbf{g}_{T^i}(\hat{p}_{\mathcal{M}}), \mathbf{g}_{T^i}(\hat{q}_{\mathcal{M}}))_{T^i} + s_{\mathcal{M}}(\hat{p}_{\mathcal{M}}, \hat{q}_{\mathcal{M}})$$

► Discrete linear form (with $\ell_{\mathcal{M}}$ defined so as to ensure consistency):

$$\ell_{\mathcal{M}}(\hat{q}_{\mathcal{M}}) := \sum_{T \in \mathcal{T}} \sum_{i \in \{1,2\}} (f, w_{T^i})_{T^i} + \sum_{T \in \mathcal{T}^{\text{cut}}} (g_N, q_{T^2})_{T^{\Gamma}} + \sum_{T \in \mathcal{T}^{\text{cut}}} \kappa_1(g_D, [\![q_T]\!] h_T^{-1} - \mathbf{g}_{T^1} \cdot \mathbf{n}_{\Gamma})_{T^{\Gamma}}$$

■ Unfitted HHO method: handling of curved interfaces in well-cut configuration
 → Need to stabilize ill-cut configurations

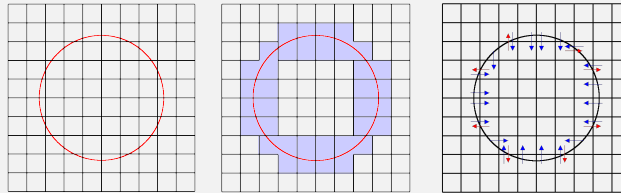
Stabilization of ill-cut cells



■ Cell agglomeration: Sollie, Bokhove, van der Vegt (2011) Johansson, Larson (2013)

- ✓ Leverages on polyhedral capacity of HHO methods → No change in numerical scheme
- ✗ Intrusive on mesh data structure

Stabilization of ill-cut cells



■ Cell agglomeration:

Sollie, Bokhove, van der Vegt (2011) Johansson, Larson (2013)

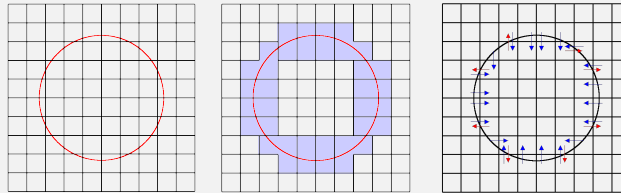
- ✓ Leverages on polyhedral capacity of HHO methods → **No change in numerical scheme**
- ✗ **Intrusive on mesh data structure**

■ Polynomial extension:

This Thesis

- ✓ Works on initial mesh (non-intrusive on mesh data structure)
- ✗ Requires modification of stencil: **intrusive at assembly level**

Stabilization of ill-cut cells



■ Cell agglomeration: Sollie, Bokhove, van der Vegt (2011) Johansson, Larson (2013)

- ✓ Leverages on polyhedral capacity of HHO methods → No change in numerical scheme
- ✗ Intrusive on mesh data structure

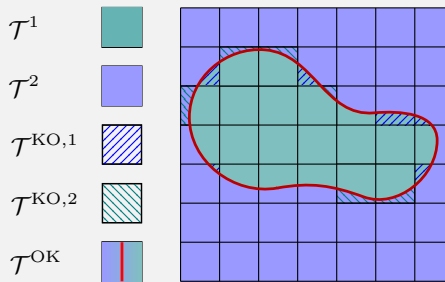
■ Polynomial extension: This Thesis

- ✓ Works on initial mesh (non-intrusive on mesh data structure)
- ✗ Requires modification of stencil: intrusive at assembly level

■ Common feature: Pairing operator

■ Mesh partitioning

$$\mathcal{T} := \mathcal{T}^{\text{uncut}} \cup \mathcal{T}^{\text{cut}}$$



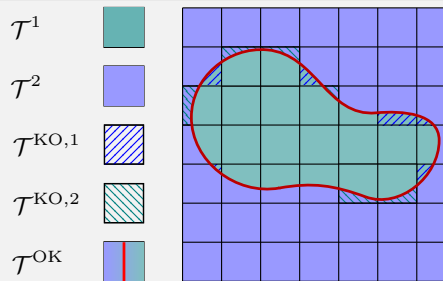
■ Mesh partitioning

$$\mathcal{T} := \mathcal{T}^{\text{uncut}} \cup \mathcal{T}^{\text{cut}}$$

$$\mathcal{T}^{\text{cut}} := \mathcal{T}^{\text{OK}} \cup \mathcal{T}^{\text{KO}}$$

■ Ball condition

- For a fixed parameter $\vartheta \in (0, 1)$: $T \in \mathcal{T}^{\text{OK}} \Rightarrow T^i$ contain a ball of radius $\vartheta h_T \quad \forall i \in \{1, 2\}$



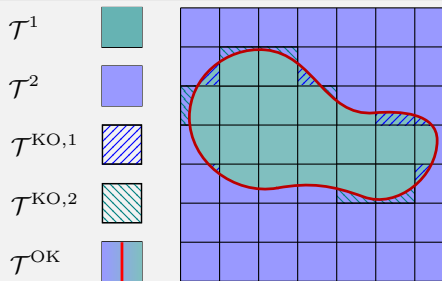
■ Mesh partitioning

$$\mathcal{T} := \mathcal{T}^{\text{uncut}} \cup \mathcal{T}^{\text{cut}}$$

$$\mathcal{T}^{\text{cut}} := \mathcal{T}^{\text{OK}} \cup \mathcal{T}^{\text{KO}} := \mathcal{T}^{\text{OK}} \cup \mathcal{T}^{\text{KO},1} \cup \mathcal{T}^{\text{KO},2}$$

■ Ball condition

- ▶ For a fixed parameter $\vartheta \in (0, 1)$: $T \in \mathcal{T}^{\text{OK}} \Rightarrow T^i$ contain a ball of radius $\vartheta h_T \quad \forall i \in \{1, 2\}$
- ▶ $\mathcal{T}^{\text{KO},1} \cap \mathcal{T}^{\text{KO},2} = \emptyset$ if mesh fine enough  Burman, Ern (2018)

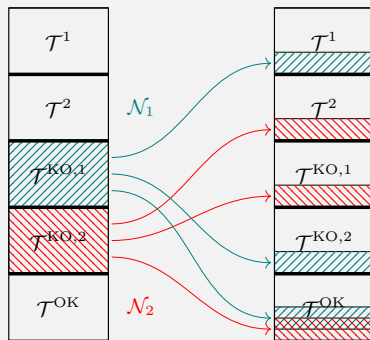


■ Pairing operator:

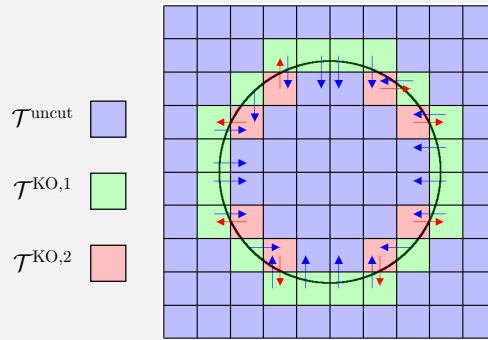
$$\mathcal{N}_i : \mathcal{T}^{\text{KO},i} \ni S \longmapsto T \in (\mathcal{T}^i \cup \mathcal{T}^{\text{OK}} \cup \mathcal{T}^{\text{KO},\bar{i}}) \cap \Delta_1(S), \quad \forall i \in \{1, 2\}$$

- $\Delta_1(S)$: first layer of neighboring cells of S

Pairing operator



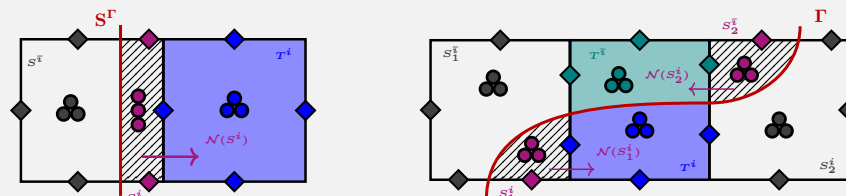
Example



III.4. Polynomial extension

■ Main idea:

- Enlarge stencil: $\hat{p}_T^{\mathcal{N}} := (\hat{p}_T, (\hat{p}_S)_{S \in \mathcal{N}^{-1}(T)}) \in \hat{P}_T^{\mathcal{N}} := \hat{P}_T^k \times \bigtimes_{S \in \mathcal{N}^{-1}(T)} \hat{P}_S^k$



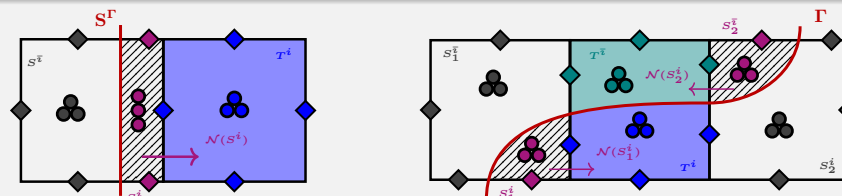
III.4. Polynomial extension

■ Main idea:

- Enlarge stencil: $\hat{p}_T^{\mathcal{N}} := (\hat{p}_T, (\hat{p}_S)_{S \in \mathcal{N}^{-1}(T)}) \in \hat{P}_T^{\mathcal{N}} := \hat{P}_T^k \times \bigtimes_{S \in \mathcal{N}^{-1}(T)} \hat{P}_S^k$
- Use ill-cut cells dofs in gradient reconstruction of **well-cut** and **uncut** (sub)cells

■ Local gradient reconstruction: If subcell T^i satisfies ball condition

$$(\mathbf{g}_{T^i}(\hat{p}_T^{\mathcal{N}}), \mathbf{q})_{T^i} := (\nabla p_{T^i}, \mathbf{q})_{T^i} + (p_{(\partial T)^i} - p_{T^i}, \mathbf{q} \cdot \mathbf{n}_T)_{(\partial T)^i} - \delta_{i1}([\![p_T]\!]_{\Gamma}, \mathbf{q} \cdot \mathbf{n}_{\Gamma})_{T^{\Gamma}} \\ + \sum_{S \in \mathcal{N}_i^{-1}(T)} \left\{ (p_{(\partial S)^i} - p_{S^i}, \mathbf{q}^+ \cdot \mathbf{n}_S)_{(\partial S)^i} - \delta_{i1}([\![p_S]\!]_{\Gamma}, \mathbf{q}^+ \cdot \mathbf{n}_{\Gamma})_{S^{\Gamma}} \right\}$$



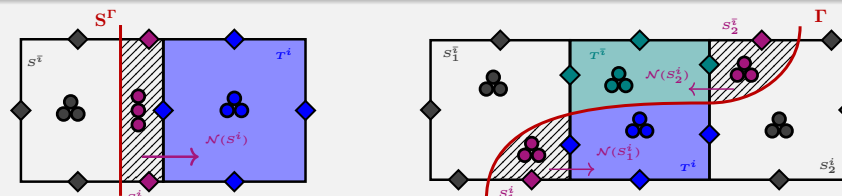
III.4. Polynomial extension

■ Main idea:

- Enlarge stencil: $\hat{p}_T^{\mathcal{N}} := (\hat{p}_T, (\hat{p}_S)_{S \in \mathcal{N}^{-1}(T)}) \in \hat{P}_T^{\mathcal{N}} := \hat{P}_T^k \times \bigtimes_{S \in \mathcal{N}^{-1}(T)} \hat{P}_S^k$
- Use ill-cut cells dofs in gradient reconstruction of **well-cut** and **uncut** (sub)cells
- Stabilize ill-cut cells dofs

■ Local gradient reconstruction: If subcell T^i satisfies ball condition

$$\begin{aligned} (\mathbf{g}_{T^i}(\hat{p}_T^{\mathcal{N}}), \mathbf{q})_{T^i} &:= (\nabla p_{T^i}, \mathbf{q})_{T^i} + (p_{(\partial T)^i} - p_{T^i}, \mathbf{q} \cdot \mathbf{n}_T)_{(\partial T)^i} - \delta_{i1}([\![p_T]\!]_{\Gamma}, \mathbf{q} \cdot \mathbf{n}_{\Gamma})_{T^{\Gamma}} \\ &\quad + \sum_{S \in \mathcal{N}_i^{-1}(T)} \left\{ (p_{(\partial S)^i} - p_{S^i}, \mathbf{q}^+ \cdot \mathbf{n}_S)_{(\partial S)^i} - \delta_{i1}([\![p_S]\!]_{\Gamma}, \mathbf{q}^+ \cdot \mathbf{n}_{\Gamma})_{S^{\Gamma}} \right\} \end{aligned}$$



■ **Stabilization:** Lehrenfeld–Schöberl stabilization & Nitsche-like penalty at interface

- ▶ Ill-cut stabilization: Direct ghost penalty on skeleton

 Preuß (2018)  Lehrenfeld, Olshanskii (2019)

$$s_{\mathcal{M}}^{\mathcal{N}}(\hat{p}_{\mathcal{M}}, \hat{q}_{\mathcal{M}}) := \sum_{(T,i) \in \mathcal{P}_h^{\text{OK}}} \sum_{S \in \mathcal{N}_i^{-1}(T)} \frac{\kappa_i}{h_S} (\underline{p}_{S^i} - p_{T^i}^+, \underline{q}_{S^i} - q_{T^i}^+)_{S^i}$$

- Connect ill-cut cell dofs with well-cut or uncut cell dofs

■ **Stabilization:** Lehrenfeld–Schöberl stabilization & Nitsche-like penalty at interface

- ▶ Ill-cut stabilization: Direct ghost penalty on skeleton

 Preuß (2018)  Lehrenfeld, Olshanskii (2019)

$$s_{\mathcal{M}}^{\mathcal{N}}(\hat{p}_{\mathcal{M}}, \hat{q}_{\mathcal{M}}) := \sum_{(T,i) \in \mathcal{P}_h^{\text{OK}}} \sum_{S \in \mathcal{N}_i^{-1}(T)} \frac{\kappa_i}{h_S} (\underline{p}_{S^i} - p_{T^i}^+, \underline{q}_{S^i} - q_{T^i}^+)_{S^i}$$

- Connect ill-cut cell dofs with well-cut or uncut cell dofs

■ **Main error estimate:** Let $p \in H^s(\Omega_1 \cup \Omega_2)$ with $s \in (\frac{3}{2}, k+2]$

$$\left\{ \sum_{T \in \mathcal{T}} \sum_{i \in \{1,2\}} \kappa_i \|\nabla(p_i - p_{T^i})\|_{T^i}^2 \right\}^{\frac{1}{2}} \lesssim h^{s-1} \sum_{i \in \{1,2\}} \kappa_i^{\frac{1}{2}} |p_i|_{H^s(\Omega_i)}$$

- ▶ Optimal convergence rates in H^1 -norm: $O(h^{k+1})$

III.5. Implementation details

- New branch in ProtoN C++ library with following features (**porting to disk++ in progress**)
 - ▶ Modal (centered and scaled) bases attached to sub-cells

III.5. Implementation details

- New branch in ProtoN C++ library with following features (**porting to disk++ in progress**)

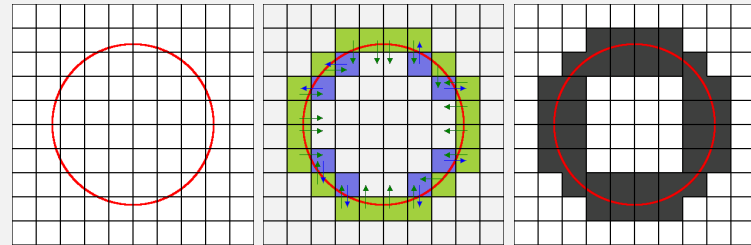
- ▶ Modal (centered and scaled) bases attached to sub-cells
- ▶ Quadratures in cut cells based on **sub-triangulation**, using a pcw. linear approximation of interface into 2^r ($r \approx 6$) **segments**

- Improvement of polynomial integration in cut cells

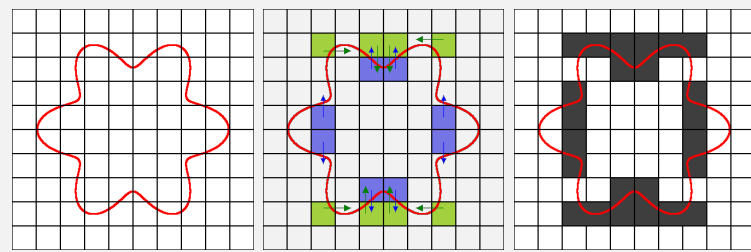
- ▶ Isoparametric description of interface  [Lehrenfeld \(2016\)](#)
- ▶ Successive integration by parts  [Antonietti, Houston, Pennesi \(2018\)](#)

III.6. Numerical results

$T \in \mathcal{T}^{\text{KO},1}$



$T \in \mathcal{T}^{\text{KO},2}$



AGGLOMERATED
CELL



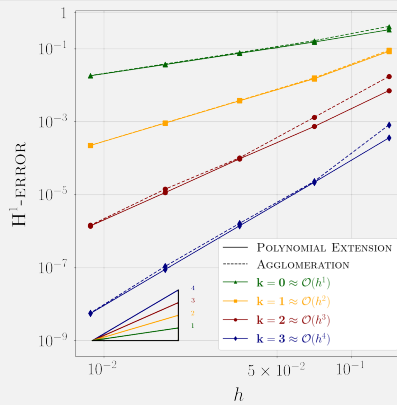
Convergence rates on smooth solutions

$$u(x, y) = \sin(\pi x) \sin(\pi y), \quad g_D = g_N = 0, \quad \kappa_1 = \kappa_2 = 1$$

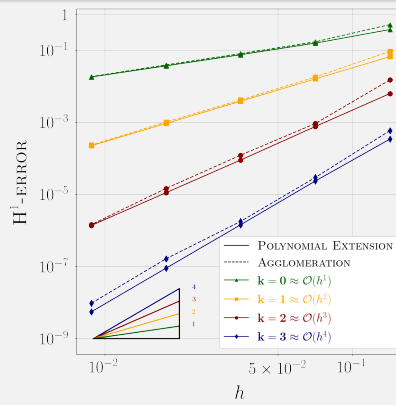
Convergence rates on smooth solutions

$$u(x, y) = \sin(\pi x) \sin(\pi y), \quad g_D = g_N = 0, \quad \kappa_1 = \kappa_2 = 1$$

Circular interface

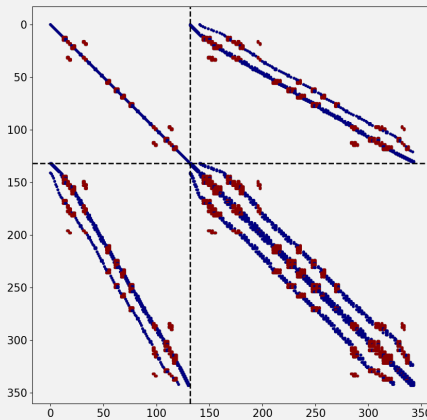


Flower-like interface

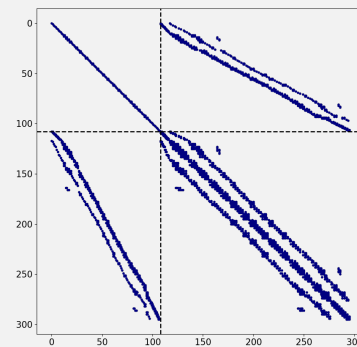


Comparison of matrix sparsity profiles

Polynomial extension



Cell agglomeration



Solutions with contrasted diffusivity

- Circular interface, no jumps ($g_D = g_N = 0$), polar coordinates (ρ, θ) :

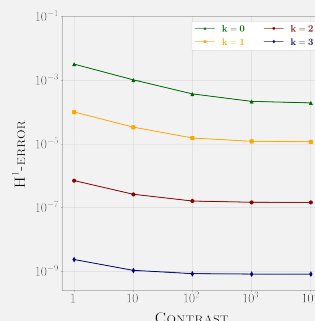
$$u_1(\rho) = \frac{\rho^6}{\kappa_1}, \quad u_2(\rho) = \frac{\rho^6}{\kappa_2} + R^6 \left(\frac{1}{\kappa_1} - \frac{1}{\kappa_2} \right)$$

Solutions with contrasted diffusivity

- Circular interface, no jumps ($g_D = g_N = 0$), polar coordinates (ρ, θ) :

$$u_1(\rho) = \frac{\rho^6}{\kappa_1}, \quad u_2(\rho) = \frac{\rho^6}{\kappa_2} + R^6 \left(\frac{1}{\kappa_1} - \frac{1}{\kappa_2} \right)$$

- H^1 -Error vs. $\kappa_2 = 10^m \kappa_1$, $r = 10$



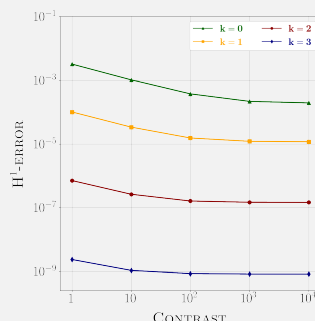
- Robustness wrt contrast

Solutions with contrasted diffusivity

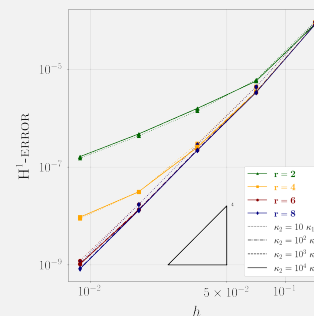
- Circular interface, no jumps ($g_D = g_N = 0$), polar coordinates (ρ, θ) :

$$u_1(\rho) = \frac{\rho^6}{\kappa_1}, \quad u_2(\rho) = \frac{\rho^6}{\kappa_2} + R^6 \left(\frac{1}{\kappa_1} - \frac{1}{\kappa_2} \right)$$

- H^1 -Error vs. $\kappa_2 = 10^m \kappa_1$, $r = 10$



- H^1 -Error vs. h , $k = 3$, $r \in \{2, 4, 6, 8\}$:



- Robustness wrt contrast

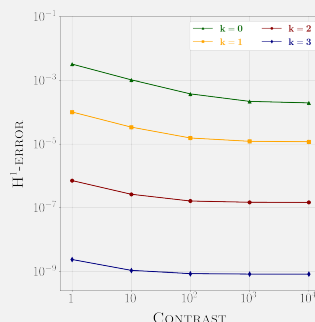
- High quality quadrature in subcell

Solutions with contrasted diffusivity

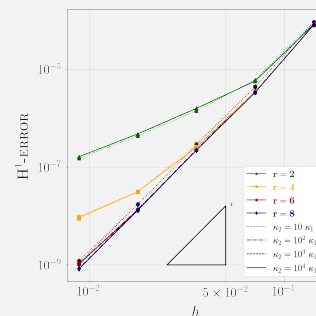
- Circular interface, no jumps ($g_D = g_N = 0$), polar coordinates (ρ, θ) :

$$u_1(\rho) = \frac{\rho^6}{\kappa_1}, \quad u_2(\rho) = \frac{\rho^6}{\kappa_2} + R^6 \left(\frac{1}{\kappa_1} - \frac{1}{\kappa_2} \right)$$

- H^1 -Error vs. $\kappa_2 = 10^m \kappa_1$, $r = 10$



- H^1 -Error vs. h , $k = 3$, $r \in \{2, 4, 6, 8\}$:



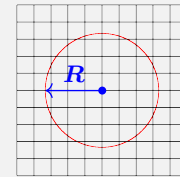
- Robustness wrt contrast

- Same conclusions for non-polynomial jumps

- High quality quadrature in subcell

Conditioning of stiffness matrix

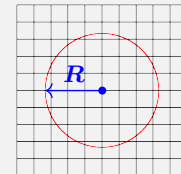
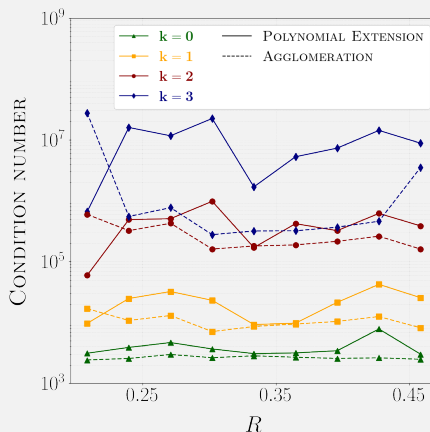
- Circular interface with radius: $R = \frac{1}{3} + \frac{i}{32}, \quad i \in \{-4, \dots, 4\}$



Conditioning of stiffness matrix

- Circular interface with radius:

$$R = \frac{1}{3} + \frac{i}{32}, \quad i \in \{-4, \dots, 4\}$$



- Grow of conditioning with polynomial degree
- Robust conditioning for circular interface

Conclusion

Summary

- **HHO:** Accurate and robust simulation of elasto-acoustic wave propagation
 - ▶ Efficient implicit and explicit time discretizations
 - ▶ Allows for **general meshes**

Conclusion

Summary

- **HHO:** Accurate and robust simulation of elasto-acoustic wave propagation
 - ▶ Efficient implicit and explicit time discretizations
 - ▶ Allows for **general meshes**
- **unfitted HHO** for elliptic interface problem
 - ▶ Novel stabilization with **polynomial extension**

Conclusion

Summary

- **HHO:** Accurate and robust simulation of elasto-acoustic wave propagation
 - ▶ Efficient implicit and explicit time discretizations
 - ▶ Allows for **general meshes**
- **unfitted HHO** for elliptic interface problem
 - ▶ Novel stabilization with **polynomial extension**

Perspectives

- Radiative boundary conditions: Robin, PML etc...  Berenger (1994)

Conclusion

Summary

- **HHO:** Accurate and robust simulation of elasto-acoustic wave propagation
 - ▶ Efficient implicit and explicit time discretizations
 - ▶ Allows for **general meshes**
- **unfitted HHO** for elliptic interface problem
 - ▶ Novel stabilization with **polynomial extension**

Perspectives

- Radiative boundary conditions: Robin, PML etc...  [Berenger \(1994\)](#)
- Extension to other physics: linear attenuation, anisotropy, poroelasticity, etc...

Conclusion

Summary

- **HHO:** Accurate and robust simulation of elasto-acoustic wave propagation
 - ▶ Efficient implicit and explicit time discretizations
 - ▶ Allows for **general meshes**
- **unfitted HHO** for elliptic interface problem
 - ▶ Novel stabilization with **polynomial extension**

Perspectives

- Radiative boundary conditions: Robin, PML etc...  [Berenger \(1994\)](#)
- Extension to other physics: linear attenuation, anisotropy, poroelasticity, etc...
- Structure-preserving RK schemes (symplectic or energy-preserving)
 [Sánchez, Cockburn, Nguyen, Peraire \(2021\)](#)

Conclusion

Summary

- **HHO:** Accurate and robust simulation of elasto-acoustic wave propagation
 - ▶ Efficient implicit and explicit time discretizations
 - ▶ Allows for **general meshes**
- **unfitted HHO** for elliptic interface problem
 - ▶ Novel stabilization with **polynomial extension**

Perspectives

- Radiative boundary conditions: Robin, PML etc...  [Berenger \(1994\)](#)
- Extension to other physics: linear attenuation, anisotropy, poroelasticity, etc...
- Structure-preserving RK schemes (symplectic or energy-preserving)
 [Sánchez, Cockburn, Nguyen, Peraire \(2021\)](#)
- **unfitted HHO** for elasto-acoustic wave propagation

Conclusion

Summary

- **HHO:** Accurate and robust simulation of elasto-acoustic wave propagation
 - ▶ Efficient implicit and explicit time discretizations
 - ▶ Allows for **general meshes**
- **unfitted HHO** for elliptic interface problem
 - ▶ Novel stabilization with **polynomial extension**

Perspectives

- Radiative boundary conditions: Robin, PML etc...  [Berenger \(1994\)](#)
- Extension to other physics: linear attenuation, anisotropy, poroelasticity, etc...
- Structure-preserving RK schemes (symplectic or energy-preserving)
 [Sánchez, Cockburn, Nguyen, Peraire \(2021\)](#)
- **unfitted HHO** for elasto-acoustic wave propagation
- **SEM-HHO coupling**

**THANK YOU FOR YOUR
ATTENTION!**

Error estimate coupling wave problem

■ Focus on acoustic subdomain

- (1) **Error equations:** For all $t \in \bar{J}$,

$$\begin{aligned}\mathbf{N}_{\mathcal{T}^F}(t) &:= \mathbf{v}_{\mathcal{T}^F}(t) - \mathbf{I}_{\mathcal{T}^F}^{H+}(\mathbf{v}(t)) \\ \hat{e}_{\mathcal{M}^F}(t) &:= \hat{p}_{\mathcal{M}^F}(t) - \hat{I}_{\mathcal{M}^F}^{HHO}(p(t))\end{aligned}$$

- ▶ **Error on dual variable:** For all $\mathbf{r}_{\mathcal{T}^F} \in \mathcal{V}_{\mathcal{T}^F}^k$,

$$(\partial_t \mathbf{N}_{\mathcal{T}^F}(t), \mathbf{r}_{\mathcal{T}^F})_{\rho^F; \Omega^F} - (\mathbf{G}_{\mathcal{T}^F}(\hat{e}_{\mathcal{M}^F}(t)), \mathbf{r}_{\mathcal{T}^F})_{\Omega^F} = (\partial_t \mathbf{v}(t) - \mathbf{I}_{\mathcal{T}^F}^{H+}(\partial_t \mathbf{v}(t)), \mathbf{r}_{\mathcal{T}^F})_{\rho^F; \Omega^F}$$

- ▶ **Error on primal variable:** For all $\hat{q}_{\mathcal{M}^F} \in \hat{\mathcal{U}}_h^F$,

$$\begin{aligned}(\partial_t e_{\mathcal{T}^F}(t), q_{\mathcal{T}^F})_{\frac{1}{\kappa}; \Omega^F} + (\mathbf{N}_{\mathcal{T}^F}(t), \mathbf{G}_{\mathcal{T}^F}(\hat{q}_{\mathcal{M}^F}))_{L^2(\Omega^F)} + s_{\mathcal{M}^F}(\hat{e}_{\mathcal{M}^F}(t), \hat{q}_{\mathcal{M}^F}) + (\mathbf{e}_{\mathcal{F}^S}(t) \cdot \mathbf{n}_\Gamma, q_{\mathcal{F}^F})_\Gamma \\ = \sum_{T \in \mathcal{T}^F} ((\mathbf{v}(t) - \mathbf{I}_T^{H+}(\mathbf{v}(t))) \cdot \mathbf{n}_T, \Pi_{\partial T}^k(q_{\partial T} - q_T))_{\partial T} - s_{\mathcal{M}^F}(\hat{I}_{\mathcal{M}^F}^{HHO}(p(t)), \hat{q}_{\mathcal{M}^F})\end{aligned}$$

Error estimate coupling wave problem

- (2) **Stability:** Testing with discrete errors, for all $t \in \overline{J}$,

$$\begin{aligned} \frac{1}{2} \frac{d}{dt} \left\{ \|e_{\mathcal{T}^F}(t)\|_{\frac{1}{\kappa}; \Omega^F}^2 + \|\mathbf{N}_{\mathcal{T}^F}(t)\|_{\rho^F; \Omega^F}^2 + \dots \right\} + s_{\mathcal{M}^F}(\hat{e}_{\mathcal{M}^F}(t), \hat{e}_{\mathcal{M}^F}(t)) + \dots \\ = (\partial_t \mathbf{m}(t) - \mathbf{I}_{\mathcal{T}^F}^{H+}(\partial_t \mathbf{m}(t)), \mathbf{N}_{\mathcal{T}^F}(t))_{\rho^F; \Omega^F} + \dots + \psi_{\mathcal{M}^F}((\mathbf{m}(t), p(t)); \hat{e}_{\mathcal{M}^F}(t)) + \dots \end{aligned}$$

- ▶ **Acoustic consistency error:**

$$\begin{aligned} \psi_{\mathcal{M}^F}((\mathbf{m}(t), p(t)); \hat{q}_{\mathcal{M}^F}) := \sum_{T \in \mathcal{T}^F} ((\mathbf{m}(t) - \mathbf{I}_T^{H+}(\mathbf{m}(t))) \cdot \mathbf{n}_T, \Pi_{\partial T}^k(q_{\partial T} - q_T))_{L^2(\partial T)} \\ - s_{\mathcal{M}^F}(\hat{I}_{\mathcal{M}^F}^{HHO}(p(t)), \hat{q}_{\mathcal{M}^F}) \end{aligned}$$

Spectral analysis

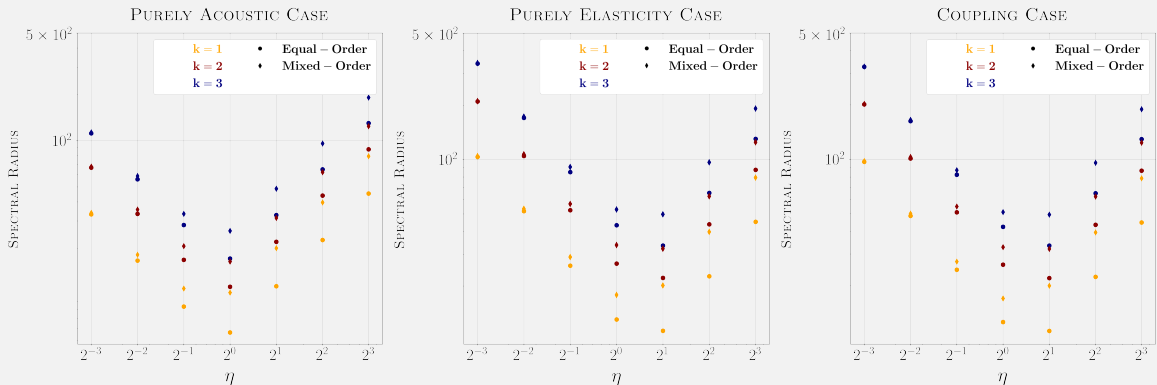


Figure 1: Spectral radius in the equal-Order and mixed-Order settings for the pure acoustic, pure linear elasticity, and elasto-acoustic coupling cases with $k \in \{1:3\}$

	$k \backslash \eta/\eta_*$	1/8	1/4	1/2	1	2	4	8
	k	1	2	3	4	5	6	7
EQUAL-ORDER	1	55.3	27.8	14.2	9.9	19.7	39.5	78.9
	2	114.8	57.8	29.5	19.5	38.3	76.3	152.5
	3	185.2	93.2	47.7	29.6	57.3	113.9	227.3
MIXED-ORDER	1	94.2	48.3	26.3	16.5	20.7	41.0	81.7
	2	195.0	99.3	53.0	31.8	33.2	64.7	128.7
	3	314.3	159.6	84.3	50.0	51.3	99.4	197.4

Table 1: Spectral radius in the equal- and mixed-order settings for the elasto-acoustic coupling with reference weights and $k \in \{1:3\}$

	SIMPLICIAL MESHES \triangle		QUADRAGULAR MESHES \square		POLYGONAL MESHES \diamond	
	EQUAL-ORDER	MIXED-ORDER	EQUAL-ORDER	MIXED-ORDER	EQUAL-ORDER	MIXED-ORDER
$k = 1$	11.6	17.6	9.9	16.5	10.5	20.1
$k = 2$	21.3	31.4	19.5	31.8	20.7	37.2
$k = 3$	33.4	47.8	29.6	50.0	35.2	59.4
$k = 4$	49.2	69.5	45.3	74.0	53.9	86.6
$k = 5$	68.0	93.7	61.5	100.6	76.6	118.9
$k = 6$	90.1	123.2	83.0	134.0	103.5	156.3

Table 2: Spectral radius for different cell geometries in equal- and mixed-order settings with $k \in \{1:6\}$ and optimal setting for η^F and η^S

Butcher tables of RK schemes

$$\begin{array}{c|cc}
 \frac{1}{4} & \frac{1}{4} & 0 \\
 \frac{3}{4} & \frac{1}{2} & \frac{1}{4} \\ \hline
 & \frac{1}{2} & \frac{1}{2}
 \end{array}
 \quad
 \begin{array}{c|ccc}
 \theta & \theta & 0 & 0 \\
 \frac{1}{2} & \frac{1}{2} - \theta & \theta & 0 \\
 1 - \theta & 2\theta & 1 - 4\theta & \theta \\ \hline
 & \xi & 1 - 2\xi & \xi
 \end{array} \tag{1a}$$

SDIRK(3,4) scheme corresponds to the values $\theta := \frac{1}{\sqrt{3}} \cos\left(\frac{\pi}{18}\right) + \frac{1}{2}$ and $\xi := \frac{1}{6(2\theta-1)^2}$

$$\begin{array}{c|cc}
 0 & 0 & 0 \\
 \frac{1}{2} & \frac{1}{2} & 0 \\ \hline
 & 0 & 1
 \end{array}
 \quad
 \begin{array}{c|ccc}
 0 & 0 & 0 & 0 \\
 \frac{1}{2} & \frac{1}{2} & 0 & 0 \\
 1 & -1 & 2 & 0 \\ \hline
 & \frac{1}{6} & \frac{2}{3} & \frac{1}{6}
 \end{array}
 \quad
 \begin{array}{c|ccccc}
 0 & 0 & 0 & 0 & 0 \\
 \frac{1}{2} & \frac{1}{2} & 0 & 0 & 0 \\
 \frac{1}{2} & 0 & \frac{1}{2} & 0 & 0 \\
 1 & 0 & 0 & 1 & 0 \\ \hline
 & \frac{1}{6} & \frac{1}{3} & \frac{1}{3} & \frac{1}{6}
 \end{array} \tag{1b}$$

Smooth analytical solution for coupling waves

- $\Omega^F := (0, 1) \times (0, 1)$, with $\rho^F := 1$, $\kappa := 1$, $c_p^F := 1$
- $\Omega^S := (-1, 0) \times (0, 1)$, with $\rho^S := 1$, $c_p^S := \sqrt{3}$, $c_s := 1$

Analytical solution is expressed in terms of u (acoustic) and $\mathbf{u} := (u_x, u_y)$ (elastic) so that

$$p := \partial_t u \quad \mathbf{m} := \nabla u \quad \text{in } \Omega^F, \quad (2a)$$

$$\mathbf{v} := \partial_t \mathbf{u} \quad \mathbb{C}^{-1} : \mathbf{s} := \nabla_{\text{sym}} \mathbf{u} \quad \text{in } \Omega^S. \quad (2b)$$

Source terms, (non)homogeneous Dirichlet boundary conditions, and initial conditions are defined according the following choices:

- Polynomial in space

$$u := (1 - x)x^2(1 - y)y \sin(\sqrt{2}\pi t) \quad u_x = u_y := (1 + x)x^2(1 - y)y \sin(\sqrt{2}\pi t); \quad (3a)$$

- Polynomial in time

$$u = u_x = u_y := x \sin(\pi x) \sin(\pi y) t^2. \quad (3b)$$

Ricker wavelet in academic test case

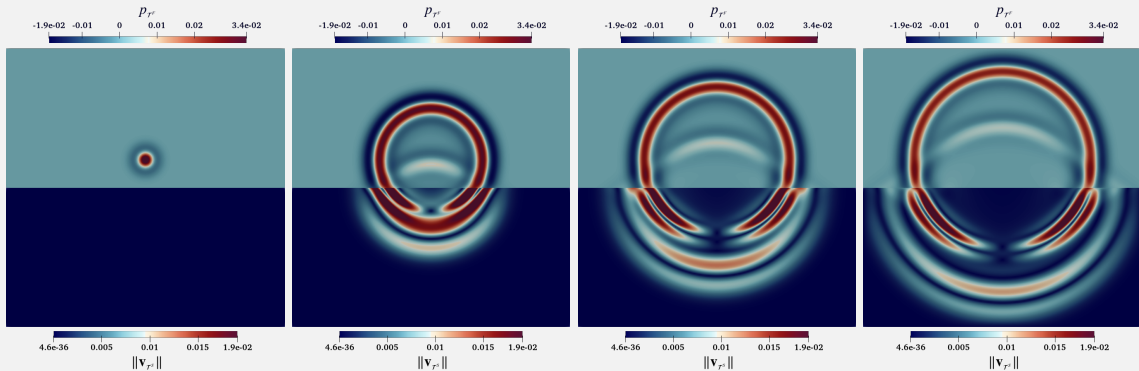


Figure 2: Spatial distribution of the acoustic pressure (upper side) and the elastic velocity norm (lower side) at times $t \in \{0, 0.25, 0.27, 0.32\}$ predicted by SDIRK(3, 4) scheme with mixed-order setting, $\mathcal{O}(\frac{1}{h})$ -stabilization, $k = 1$, $\ell = 7$, and $n = 9$.

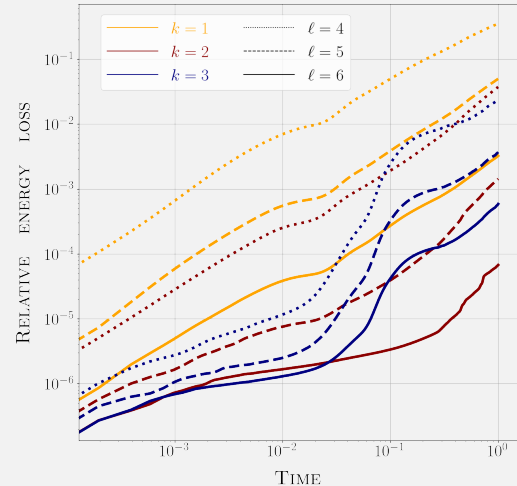
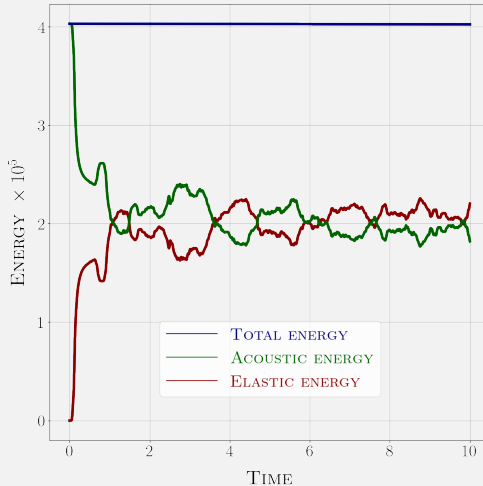


Figure 3: SDIRK(3,4) scheme with $n = 9$. **Left:** Energy repartition as a function of the time for $k = 3$ and $\ell = 6$. **Right:** Relative energy loss as function of the time for $k \in \{1, 2, 3\}$ and $\ell \in \{4, 5, 6\}$.

CFL stability limit

$$u(t, x, y) := x^2 \sin(\omega\pi x) \sin(\omega\pi y) \sin(\theta\pi t),$$

$$u_x(t, x, y) = u_y(t, x, y) := x^2 \cos(\omega\frac{\pi}{2}x) \sin(\omega\pi y) \cos(\theta\pi t),$$

- Dominant spatial evolution: $\omega := 5$ and $\theta := \sqrt{2}$
- Dominant temporal evolution: $\omega := 1$ and $\theta := 10$

Algorithm 1: Bounding of the CFL Stability Limit

```

1 while simulation is stable do
2   for n = 1 to N do
3     Compute energy  $E_n$ ;
4     Compute relative energy increase  $\Delta E := \max_n \left( \frac{|E_n - E_0|}{E_0}, \frac{|E_n - E_{n-1}|}{E_{n-1}} \right)$ ;
5     if  $\Delta E > \varepsilon$  then
6       Flag N as the first unstable time step;
7       break;
8   Flag N as the last stable time step;
9   Decrease N by  $\delta N$ ;

```

	$k = 1$			$k = 2$			$k = 3$		
	$s = 2$	$s = 3$	$s = 4$	$s = 2$	$s = 3$	$s = 4$	$s = 2$	$s = 3$	$s = 4$
CFL*	0.205	0.253	0.282	0.099	0.123	0.138	0.063	0.079	0.087
RATIO WRT s	1	1.23	1.38	1	1.24	1.39	1	1.25	1.38
RATIO WRT k	1	1	1	0.48	0.49	0.49	0.31	0.31	0.31

Table 3: CFL* coefficient (and ratios thereof) for ERK(s), $s \in \{2, 3, 4\}$ and $k \in \{1, 2, 3\}$.

MESHES	$s = 2$			$s = 3$			$s = 4$			
	\triangle	\square	\diamond	\triangle	\square	\diamond	\triangle	\square	\diamond	
$k = 1$	CFL*	0.191	0.205	0.264	0.238	0.253	0.329	0.265	0.282	0.363
	RATIO	1	1.07	1.38	1	1.06	1.38	1	1.06	1.37
$k = 2$	CFL*	0.106	0.099	0.136	0.133	0.123	0.170	0.147	0.138	0.188
	RATIO	1	0.93	1.28	1	0.92	1.28	1	0.94	1.28
$k = 3$	CFL*	0.072	0.063	0.082	0.090	0.079	0.102	0.100	0.087	0.115
	RATIO	1	0.88	1.13	1	0.88	1.13	1	0.87	1.15

Table 4: CFL* coefficient (and ratios thereof) for ERK(s), $s \in \{2, 3, 4\}$ and $k \in \{1, 2, 3\}$.

Efficiency study

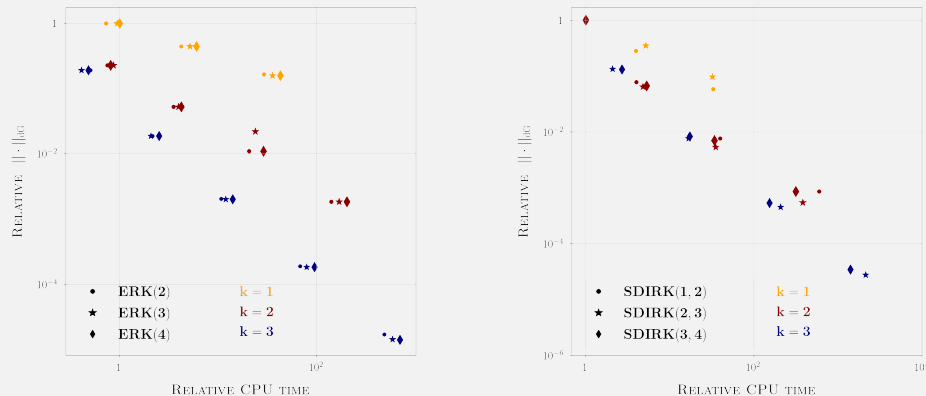


Figure 5: Test case with dominant spatial error. **Left panel:** Efficiency comparison for ERK(s) for $s \in \{2, 3, 4\}$. **Right panel:** Efficiency for SDIRK($s, s + 1$) for $s \in \{1, 2, 3\}$.

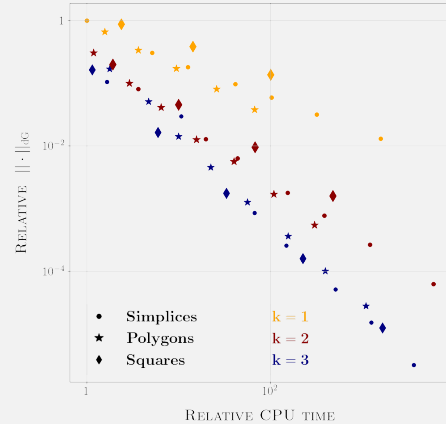
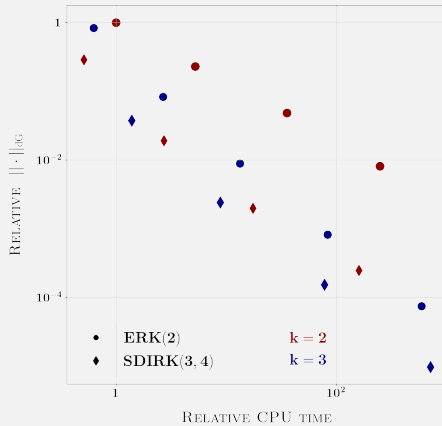


Figure 6: Test case with dominant spatial error. **Left panel:** Efficiency comparison for ERK(2) and SDIRK(3,4). **Right panel:** Efficiency comparison for ERK(4) on meshes composed of different cell geometries.

Coupling condition

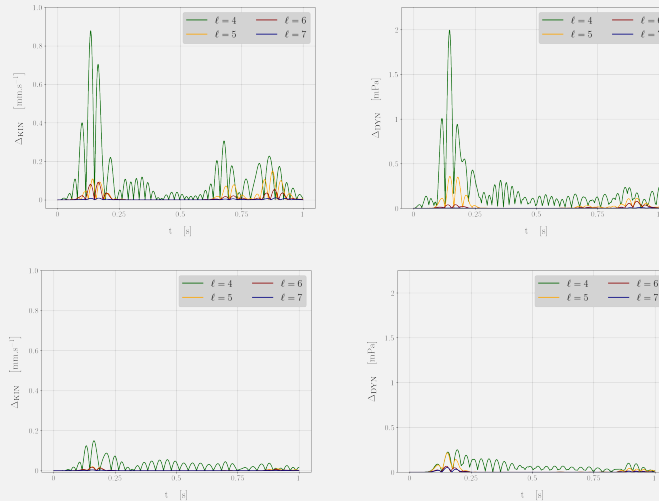


Figure 7: Errors on the coupling conditions as a function of the time predicted by SDIRK(3,4) for $k = 1$ (top row) and $k = 3$ (bottom row). **Left:** Kinematic errors. **Right:** Dynamic errors.

Efficiency study on Ricker wavelet

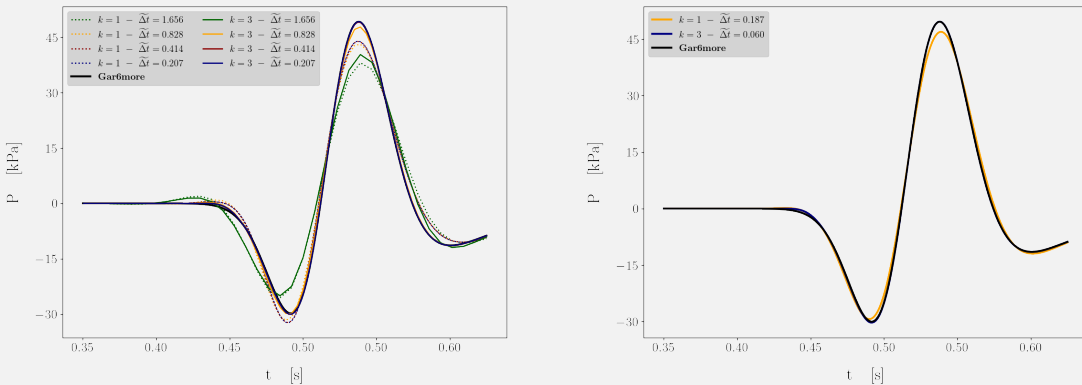


Figure 8: Spatial distribution of the acoustic pressure at \mathcal{S}^F at times $t \in [0, 0.625][\text{s}]$. **Left column:** SDIRK(3,4), $k \in \{1, 3\}$, and $\tilde{\Delta}t \in \{0.402, 0.805, 1.609, 3.219\}$. **Right column:** ERK(4), $k \in \{1, 3\}$ and $\tilde{\Delta}t = \{0.117, 0.363\}$ (recall that $\text{CFL}^* = 0.087$ for $k = 3$).

▲ What happen in ill-cut cells ?

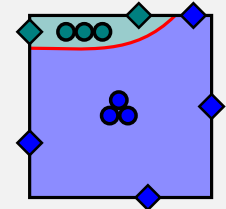
- Discrete trace inequality:

$$\|p_{T^i}\|_{(\partial T)^i} + \|p_{T^i}\|_{T^\Gamma} \lesssim C_{\text{TRACE}} h_T^{-\frac{1}{2}} \|p_{T^i}\|_{T^i},$$

- ▶ C_{TRACE} degenerate
- Stability and boundedness: For all $\hat{p}_T \in \hat{P}_T$,

$$|||\hat{p}_T|||^2 \lesssim a_T(\hat{p}_T, \hat{p}_T) \lesssim |||\hat{p}_T|||^2 := \|\nabla p_T\|_{T^i}^2 + h_T^{-1} \|p_T - p_{\partial T}\|_{(\partial T)^i}^2$$

- ▶ Not true anymore



■ Stabilization:

- ▶ Keep Lehrenfeld–Schöberl stabilization & Nitsche-like penalty at interface:

$$s_{\mathcal{M}}^{\circ}(\hat{p}_{\mathcal{M}}, \hat{q}_{\mathcal{M}}), \quad s_{\mathcal{M}}^{\Gamma}(\hat{p}_{\mathcal{M}}, \hat{q}_{\mathcal{M}})$$

- ▶ Ill-cut stabilization: Direct ghost penalty Preuß (2018) Lehrenfeld, Olshanskii (2019)

$$s_{\mathcal{M}}^{\mathcal{N}}(\hat{p}_{\mathcal{M}}, \hat{q}_{\mathcal{M}}) := \sum_{(T,i) \in \mathcal{P}_h^{\text{OK}}} \sum_{S \in \mathcal{N}_i^{-1}(T)} \frac{\kappa_i}{h_S^2} (p_{S^i}^+ - p_{T^i}, q_{S^i}^+ - q_{T^i})_{T^i}$$

- Connect ill-cut cell dofs with well-cut or uncut cell dofs

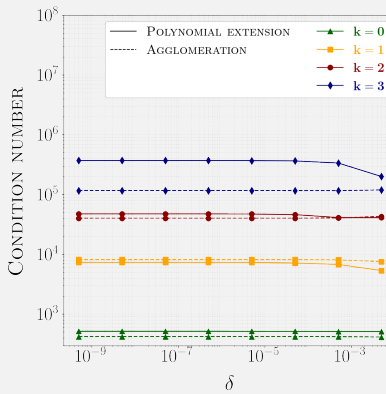
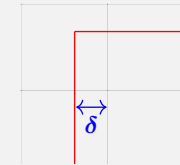
- ▶ Total stabilization:

$$s_{\mathcal{M}}(\hat{p}_{\mathcal{M}}, \hat{q}_{\mathcal{M}}) := s_{\mathcal{M}}^{\circ}(\hat{p}_{\mathcal{M}}, \hat{q}_{\mathcal{M}}) + s_{\mathcal{M}}^{\Gamma}(\hat{p}_{\mathcal{M}}, \hat{q}_{\mathcal{M}}) + s_{\mathcal{M}}^{\mathcal{N}}(\hat{p}_{\mathcal{M}}, \hat{q}_{\mathcal{M}})$$

Conditioning of stiffness matrix

- Square interface with distance to mesh:

$$\delta = 0.5 \times 10^{-p}, \quad p \in \{1, \dots, 9\}$$



- Grow of conditioning with polynomial degree
- **Robust conditioning** for severe ill-cut configurations

Pairing criteria

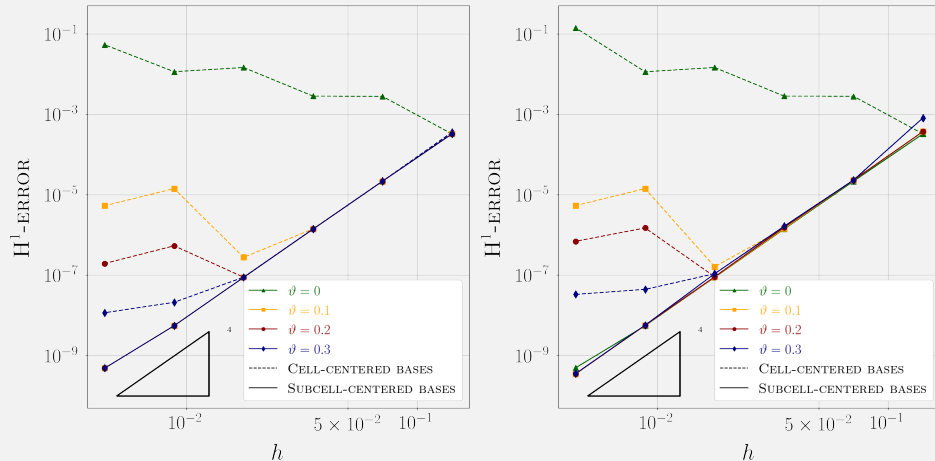


Figure 9: Errors as a function of the mesh size for the exact solution for $k = 3$ and various values of the pairing parameter ϑ used for flagging ill-cut cells. Left: polynomial extension. Right: cell agglomeration.

Convergence tests with high contrast property

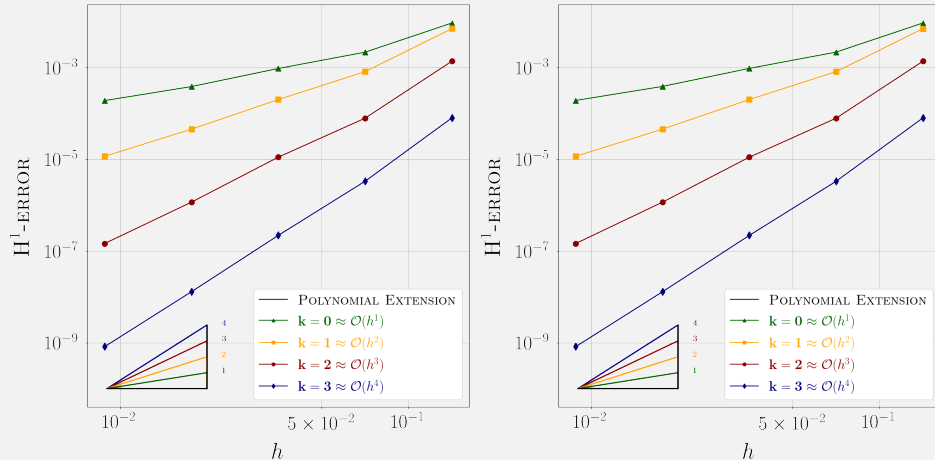


Figure 10: Errors as a function of the mesh size for the exact solution (left) and the exact solution (right) for various polynomial degrees $k \in \{0, \dots, 3\}$; diffusivity contrast set to $\kappa_2 = 10^4 \kappa_1$.

Convergence tests for non polynomial solution

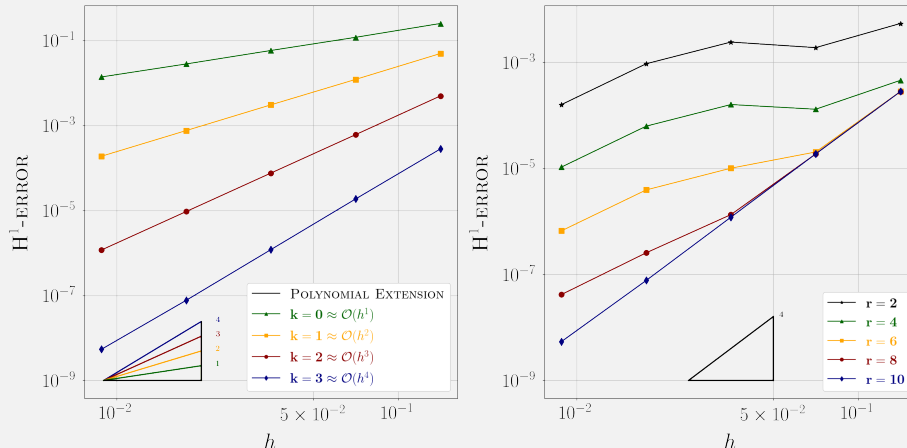


Figure 11: Left: Errors as a function of the mesh size for the exact solution for various polynomial degrees $k \in \{0, \dots, 3\}$ (with sub-triangulation parameter set to $r = 10$). Right: Errors as a function of the mesh size for $k = 3$ and $r \in \{2, 4, 6, 8, 10\}$. No diffusivity contrast.